Available online at www.sciencedirect.com

ScienceDirect

journal homepage: www.elsevier.com/locate/he

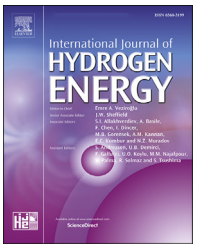

Recent advances in membrane technologies for hydrogen purification

Gabriel Bernardo [a], *Tiago Araújo* [a], *Telmo da Silva Lopes* [a], *José Sousa* [a,b], *Adélio Mendes* [a,*]

[a] *LEPABE, Department of Chemical Engineering, University of Porto, 4200-465, Porto, Portugal*

[b] *Chemistry Department, University of Trás-os-Montes e Alto Douro, Apartado 1013, 5001-801, Vila Real Codex, Portugal*

HIGHLIGHTS

Advantages and challenges of hydrogen membrane-based separation and purification process using:

- Carbon molecular sieve membranes.
- Ionic-liquid based membranes.
- Palladium-based membranes.
- Electrochemical hydrogen pumping membranes.

ARTICLE INFO

Article history:
Received 4 March 2019
Received in revised form
13 June 2019
Accepted 18 June 2019
Available online xxx

Keywords:
Hydrogen purification
Carbon molecular sieve membranes
Ionic-liquid based membranes
Palladium-based membranes
Electrochemical hydrogen pumping membranes

ABSTRACT

Planet Earth is facing accelerated global warming due to greenhouse gas emissions from human activities. The United Nations agreement at the Paris Climate Conference in 2015 highlighted the importance of reducing CO_2 emissions from fossil fuel combustion. Hydrogen is a clean and efficient energy carrier and a hydrogen-based economy is now widely regarded as a potential solution for the future of energy security and sustainability. Although hydrogen can be produced from water electrolysis, economic reasons dictate that most of the H_2 produced worldwide, currently comes from the steam reforming of natural gas and this situation is set to continue in the foreseeable future. This production process delivers a H_2-rich mixture of gases from which H_2 needs to be purified up to the ultra-high purity levels required by fuel cells (99.97%). This driving force pushes for the development of newer H_2 purification technologies that can be highly selective and more energy efficient than the traditional energy intensive processes of pressure swing adsorption and cryogenic distillation. Membrane technology appears as an obvious energy efficient alternative for producing the ultra-pure H_2 required for fuel cells. However, membrane technology for H_2 purification has still not reached the maturity level required for its ubiquitous industrial application. This review article covers the major aspects of the current research in membrane separation technology for H_2 purification, focusing on four major types of emerging membrane technologies (carbon molecular sieve membranes; ionic-liquid based membranes; palladium-based membranes and electrochemical hydrogen pumping membranes) and establishes a comparison between them in terms of advantages and limitations.

* *Corresponding author.*
E-mail address: mendes@fe.up.pt (A. Mendes).

https://doi.org/10.1016/j.ijhydene.2019.06.162

Acronyms

BCC	Body-centred cubic
BMIM	1-Butyl-3-methylimidazolium
CI	Colloid impregnation
CMSM	Carbon molecular sieve membrane
CrPSSA	Cross-linked poly(styrene sulfonic acid)
DFT	Density functional theory
DSC	Differential scanning calorimetry
EHP	Electrochemical hydrogen pumping
EHPM	Electrochemical hydrogen pumping membranes
ELP	Electroless plating
EMIM	1-Ethyl-3-methylimidazolium
FCC	Face-centred cubic
FFV	Fractional free volume
HNT	Halloysite nanotubes
IL	Ionic Liquid
IP	Impregnation-Precipitation
MFI	Mordenite Framework Inverted
NCC	Nanocrystalline cellulose
P(VDF-HFP)	Poly(vinylidene fluoride-co-hexafluoropropylene)
PBI	Poly(benzimidazole)
PEG	Poly(ethylene glycol)
PEI	Polyetherimide
PEM	Proton exchange membrane
PEMFC	Proton exchange membrane fuel cell
PF	Phenolic resin
PFNR	Phenol formaldehyde novolac resin
PFSA	Perfluorinated sulfonic acid
PI	Polyimide
PILM	Poly(ionic) liquid membrane (or polymerized ionic liquid membrane)
PPO	Poly (2,6-dimethyl-1,4-phenylene oxide)
PSA	Pressure swing adsorption
PSS	Porous stainless steel
PVDF	Polyvinylidene fluoride
PVP	Polyvinylpyrrolidone
SBA-15	Mesoporous silica
SEM	Scanning electron microscopy
SILM	Supported ionic liquid membranes
SMR	Steam methane reforming
SPEEK	Sulfonated poly(ether-ether-ketone)
SPPESK	Sulfonated poly (phthalazinone-ether-sulfone-ketone)
WGS	Water-gas shift

Introduction

Some of the most serious challenges currently facing our planet and posing serious threats to mankind are the CO_2 greenhouse global warming and its associated adverse effects [1–3], and the prospect of a global fossil fuel reserves depletion by the end of this century [4–6]. These challenges create an emergency for new and clean energy technologies that can stop or slow down the climate change and secure a global energy security based on sustainable and renewable energy sources. Owing to rapid recent advances in proton-exchange membrane fuel cell technology [7–9], hydrogen is now widely regarded as a future clean energy vector, *i.e.* a future energy solution for the 21st century and fuel of the post petroleum era [10,11]. Hydrogen will allow to reduce the threat of global warming while simultaneously guaranteeing the sustainability and security of energy.

Hydrogen, unlike coal, gas or oil, however, is not a primary energy source. Rather, it must first be produced using energy from another source and then transported for future use where its latent chemical energy can be fully exploited. Hydrogen can be obtained from diverse resources [12–16], including non-renewable (coal [17], natural gas [18] and nuclear [19]) and renewable (biomass [20–22]; water splitting using hydroelectric, solar [23], wind and geothermal energy). This diversity of supply sources will guarantee the security of energy supply largely contributing to hydrogen being such a promising energy carrier [24].

In the future, if the so called "hydrogen economy" [25–28] is to be implemented, it is envisaged that hydrogen will be stored as a fuel and used in power generation systems for stationary and mobile applications using fuel cells, internal combustion engines or turbines, with the only by-product at the point of use being water. The main advantages of the "hydrogen economy" will include: (i) the elimination of greenhouse gases and pollution caused by fossil fuels; (ii) energy security and elimination of the world's energy dependence on the fossil fuel reserves from the Middle East. The topic of hydrogen economy is currently high on the political agenda and many countries are elaborating roadmaps for the advancement of fuel cell and hydrogen technologies. However, before a hydrogen economy can be implemented, there are still many technological hurdles that must be addressed, and one of the most pressing questions that immediately arises is: how to produce the huge amounts of H_2 needed for implementing the hydrogen economy? [29].

Currently there exist in the world three main industrial methods for producing hydrogen, namely: steam methane reforming (SMR), coal and biomass gasification and water electrolysis.

In SMR H_2 is produced from a CH_4 source, such as natural gas, using high-temperature (700 °C – 1000 °C) and high pressure (3–25 bar) steam [30–37]. CH_4 reacts with steam in the presence of a catalyst (most commonly Ni-based catalyst) to produce H_2, CO and CO_2. After this step, CO reacts with steam in the so-called water-gas shift (WGS) reaction [38,39], using a catalyst (traditionally iron-chromium and copper-zinc catalysts for high and low temperatures, respectively [40]), to produce CO_2 and more H_2. In a final process step, H_2 is purified by removing CO_2 and other impurities from the gas stream.

In the gasification process [41–47], H_2 is produced by first reacting various possible feedstocks such as coal, biomass or municipal solid waste with steam or oxygen under high pressures and temperatures to form syngas, a mixture that may contain a variety of other components besides H_2, CO and CO_2 such as water vapour, small amounts of sulfur

Please cite this article as: Bernardo G et al., Recent advances in membrane technologies for hydrogen purification, International Journal of Hydrogen Energy, https://doi.org/10.1016/j.ijhydene.2019.06.162

compounds (H_2S, COS), some ammonia and other trace contaminants. The CO then reacts with H_2O to form CO_2 and more H_2 via a WGS reaction and finally the H_2 produced is purified.

In the electrolysis of water [48–52], electricity is used to split H_2O molecules into pure H_2 and O_2. Contrary to the other hydrogen production methods, the electrolysis does not require any purification step, and the H_2 produced has the advantage of being "green" or CO_2 neutral.

The electrolysis of water is the most environmentally friendly method of producing H_2, but it currently only accounts for ~4% of the global hydrogen production in the world because it is still regarded as too expensive [51], given the ample supply of fossil fuels that is expected to continue over the next decades. By contrast, the steam reforming of natural gas is the most economical and by far the most common method of producing H_2, at a scale large enough to satisfy industrial demand, accounting for more than 80% of the current world production. Due to these economic constraints, hydrogen production methods based on fossil fuels are regarded as necessary and good temporary options to follow during the transition from a carbon-based (fossil fuel) economy to a hydrogen-based economy. Therefore, and according to many projections, in the foreseeable future it is expectable that these carbon-based H_2 production methods, used in combination with CO_2 sequestration methods, will play an important role in the early period of development of the hydrogen economy [53]. For example, fuel cell electric vehicles are now being developed by some of the major car companies in the world. However, most of these cars will use hydrogen produced from fossil fuels because this is still the cheapest [54].

As mentioned above, the H_2 production methods based on SMR and gasification involve a final H_2 purification step in which CO_2 and other impurities are removed from the hydrogen gas. This final H_2 purification step is of the uttermost importance for the implementation of the hydrogen economy because polymer electrolyte membrane (PEM) fuel cells require ultra-high-purity hydrogen (mole fraction $\geq$ 99.97% and CO $\leq$ 0.2 ppm [55]) and, furthermore, the majority of other hydrogen applications (such as general industrial applications, hydrogenation and water chemistry) also need high levels of hydrogen purity ($\geq$99.95%) [56]. At this point it is worth noting that the extremely high-purity requirement of PEMs stems from the fact that PEMs use platinum-based catalysts which are extremely sensible to poisoning by contaminants such as CO and H_2S. For this reason, the interest in the production of ultra-high-purity hydrogen has strongly increased in recent years and this has placed pressure on the development of alternative methods of hydrogen purification.

Currently, the most commonly used technologies for hydrogen purification are pressure swing adsorption (PSA) [57–61], cryogenic distillation [62–64] and amine-based absorption for CO_2 removal from H_2 [65].

PSA relies on the selective adsorption of impurities from a gas stream and is the most used conventional technique. The main advantage of PSA is its ability to filter out impurities down to parts per million (ppm) producing hydrogen with high purities > 99.999%. Its main disadvantage is the high H_2 loss (~20%) resulting from the pressure release during desorption (H_2 recovery ~80%). PSA can be used for large and medium industrial scales as well as for small scale portable systems. Examples of the latter are the PSA units by companies such as HyGear, IGS and Amnis Pura that when coupled with steam methane reformers can produce PEMFC grade hydrogen. These companies offer PSA systems ranging from 10 Nm^3/h up to 1000 Nm^3/h with a H_2 purity range 99.5%–99.9999%.

Cryogenic distillation relies on the partial condensation of gas mixtures, at low temperatures and high pressures, to be separated by distillation. One major disadvantage is the limited purity levels (~99%) of the extracted hydrogen. The process is very expensive as it requires the use of numerous equipment and devices. Cryogenic distillation is ideal for large industrial scales, but unsuitable for small portable applications.

PSA and more notably cryogenic distillation involve high equipment cost and high energy consumption being therefore very expensive methods. For this reason, the H_2 purification step currently accounts for ~50% of the overall price of H_2 production using SMR and gasification. Therefore, although the steam reforming and gasification are considerably less-expensive than electrolysis, they can still be made cheaper if cheaper methods of H_2 purification can be developed.

In this context, membrane separation technology appears as an emerging and very promising industrial process, that will be able to compete and eventually replace the traditional separation techniques, due to its many associated advantages [66]. A membrane is a physical solid barrier between two phases (gaseous or liquid), with a certain perm-selectivity towards one or more components of a mixture. In gas separation applications, the force that normally drives the different species to permeate a membrane is the partial pressure difference between both sides of the membrane. An applied electrical potential difference is another possible driving force. Compared to traditional separation processes, membrane technology will be able to offer: simpler operation; higher adaptability; compactness and lightweight; modular design with simpler up- and down-scaling; lower labour intensity; lower capital, operating and maintenance costs; higher energy efficiency and a much lower environmental impact, among other advantages. Furthermore, H_2 permselective membranes, when used in membrane reactors, *i.e.* innovative integrated systems in which both reaction and separation are carried out in the same equipment, have the ability to improve yields of fuel conversion owing to the shifting of reaction equilibrium conditions. The typical target values of membrane performance that, in general, are considered necessary for the industrial purification of hydrogen are: permeability to $H_2 \geq$ 1000 Barrer and selectivity (H_2/X) $\geq$ 100.

In this review we focus on four emerging membrane separation technologies which, compared to the currently leading technologies (such as PSA, cryogenic separation and amine absorption), have the potential to be more environmentally friendly and more economically competitive, but are not yet as matured as those. These membranes technologies are: carbon molecular sieve membranes (CMSM); poly (ionic) liquid membranes (PILM) membranes; metal membranes and electrochemical hydrogen pumping membranes (EHPM).

Please cite this article as: Bernardo G et al., Recent advances in membrane technologies for hydrogen purification, International Journal of Hydrogen Energy, https://doi.org/10.1016/j.ijhydene.2019.06.162

Carbon molecular sieve membranes

General overview

Carbon molecular sieve membranes (CMSM) are produced through the carbonization of polymeric precursors at high temperatures and under a controlled atmosphere. The simple thermal treatment method for producing CMSMs was first proposed in 1980, in a seminal work by Koresh and Soffer [67], and since then these membranes have been extensively investigated for gas separation applications, including hydrogen purification. They possess high corrosion resistance, high thermal stability and excellent permeabilities and perm-selectivities, when compared to polymeric membranes. The CMSM structure is turbostratic and described as "slit-like" with a bimodal pore size distribution with micropores connecting ultramicropores [68,69]. Micropores provide sorption sites while ultramicropores (called constrictions) are the responsible for the molecular sieving mechanism of gas permeation observed in this type of membranes [70].

The high potential of CMSMs for use in the separation and purification of hydrogen from, for example, coal- and biomass-derived syngas has been recently demonstrated in a field evaluation study [71]. In another study, the techno-economic feasibility of CMSMs for H_2 purification has been demonstrated by He et al. [72] who proposed a novel, energy efficient two-stage carbon membrane system for the purification of H_2 produced from biomass fermentation. The designed two stage system can capture CO_2 > 95 vol% in the first stage operating at 20 bar and 120 °C, and retain >95% of H_2 with high purity (>99.5%) in the second, operating at a feed operation pressure of 20 bar and a low temperature of 20 °C. Based on process simulation and cost estimation, the proposed two-stage system can provide an H_2 purification cost of <1 $/kg.

In this section, we review the most important studies of CMSMs, targeting their application in the purification of H_2. Despite some existing literature reviews on CMSMs [73–75], a review focused on their application for H_2 purification is still missing. As a benchmark for high performance, we will focus on CMSMs with separation performances above the Robeson upper bound limit. Fig. 1 and Table S1 in Supporting Information summarize the most relevant H_2/X separation performances (permeability to H_2; H_2/X ideal selectivity) reported in the literature using CMSMs, where X = CH_4, N_2, O_2 and CO_2.

CMSM properties can be tuned by controlling the sorption and diffusion characteristics of the membranes. Various general strategies have been tested, by a large number of research groups, that have proved efficient at tuning and improving the hydrogen separation performance of CMSMs. These strategies include: i) changing the carbonization conditions (gas atmosphere; heating rate and dwell periods; thermostabilization temperature; carbonization end temperature); ii) pre-treatment of the precursor solution by polymer blending, or addition of nanoparticle fillers and additives; iii) post-treatments of the membranes (natural aging; aging with oxidative atmosphere) and iv) substrate surface modification.

Effect of carbonization conditions

The effect of the carbonization conditions (temperature, heating rate, and atmosphere) on the nanostructure and gas separation performance of CMSMs has been addressed in a large number of research works. For example, Suda et al. [76] studied these on CMSMs prepared from polyimide (PI) film. The carbonization end temperature was found to have the greatest impact on the microstructure and gas permeation properties of the CMSMs: increasing the pyrolysis temperature, the permeabilities to the selected gases decrease whereas the perm-selectivities to those gases increase. The membrane carbonized under Ar flow with the slowest heating rate of 1.33 °C/min exhibited the highest selectivity of all the membranes studied (H_2/N_2 = 4700) (membranes 1A-1C in Fig. 1 and Table S1). Liu et al. [77] found the temperatures of thermostabilization (400–490 °C) and carbonization (650–850 °C), in argon, to have a large effect on the permeability and selectivity to gases of the CMSMs prepared from a polymeric precursor of poly (phthalazinone ether sulfone ketone). The CMSMs thermo-stabilized at 460 °C and carbonized at 850 °C presented the highest selectivities for pure gases with an ideal H_2/N_2 selectivity of 129 (membranes 2A, 2B in Fig. 1 and Table S1). A similar study was performed by Campo et al. [78], on CMSMs prepared from a commercial film of cellophane paper as precursor. The permeabilities reached a maximum for CMSM heated up to 550 °C, without significantly compromising selectivities. The membranes heated up to 550 °C with different soaking times (Celo550-ST60; Celo550-ST240; Celo550-ST480) all overtook the Robeson upper bound for polymeric membranes, especially regarding the ideal selectivities of pairs H_2/O_2, H_2/CO_2 and H_2/CH_4, (membranes 3A-3D in Fig. 1 and Table S1). Rodrigues et al. [79] studied the impact of the carbonization end temperature on the performance of CMSMs prepared by carbonization, on α-alumina supports, of a resorcinol–formaldehyde resin loaded with boehmite. The CMSM prepared at 550 °C surpassed the Robeson upper bound for the pair H_2/N_2 (membranes 4A, 4B in Fig. 1 and Table S1). Llosa Tanco et al. [80] prepared CMSMs over asymmetric porous α-alumina support tubes by carbonization, at 500 °C under N_2 atmosphere, of a novolac phenolic resin loaded with boehmite nanoparticles. Aging of the membranes for 24 h caused a considerable decrease on the permeability to N_2 but not on the permeability to H_2. The performance, at room temperature, of the aged membranes for H_2/N_2 separation was above the Robeson upper bound limit, namely $P(H_2)$ = 140 Barrer and selectivity H_2/N_2 = 117 (membrane 5 in Fig. 1 and Table S1). In a continuation of this work [81], the same authors found the pore sizes to decrease with the carbonization temperature up to 1000 °C. Freshly prepared membranes showed high gas permeation that quickly decreased upon contacting with room atmosphere, due to the adsorption of air humidity on the pore network. After 1-day in contact with atmospheric air, the membrane carbonized at 550 °C showed an H_2/N_2 selectivity of 725 and a permeability to H_2 of 1450 Barrer at room temperature, performing above the Robeson upper bound. Heating from 100 °C to 200 °C regenerated the gas permeation of aged membranes most likely due to the removal of physically adsorbed water (membranes 6A-6E in

Please cite this article as: Bernardo G et al., Recent advances in membrane technologies for hydrogen purification, International Journal of Hydrogen Energy, https://doi.org/10.1016/j.ijhydene.2019.06.162

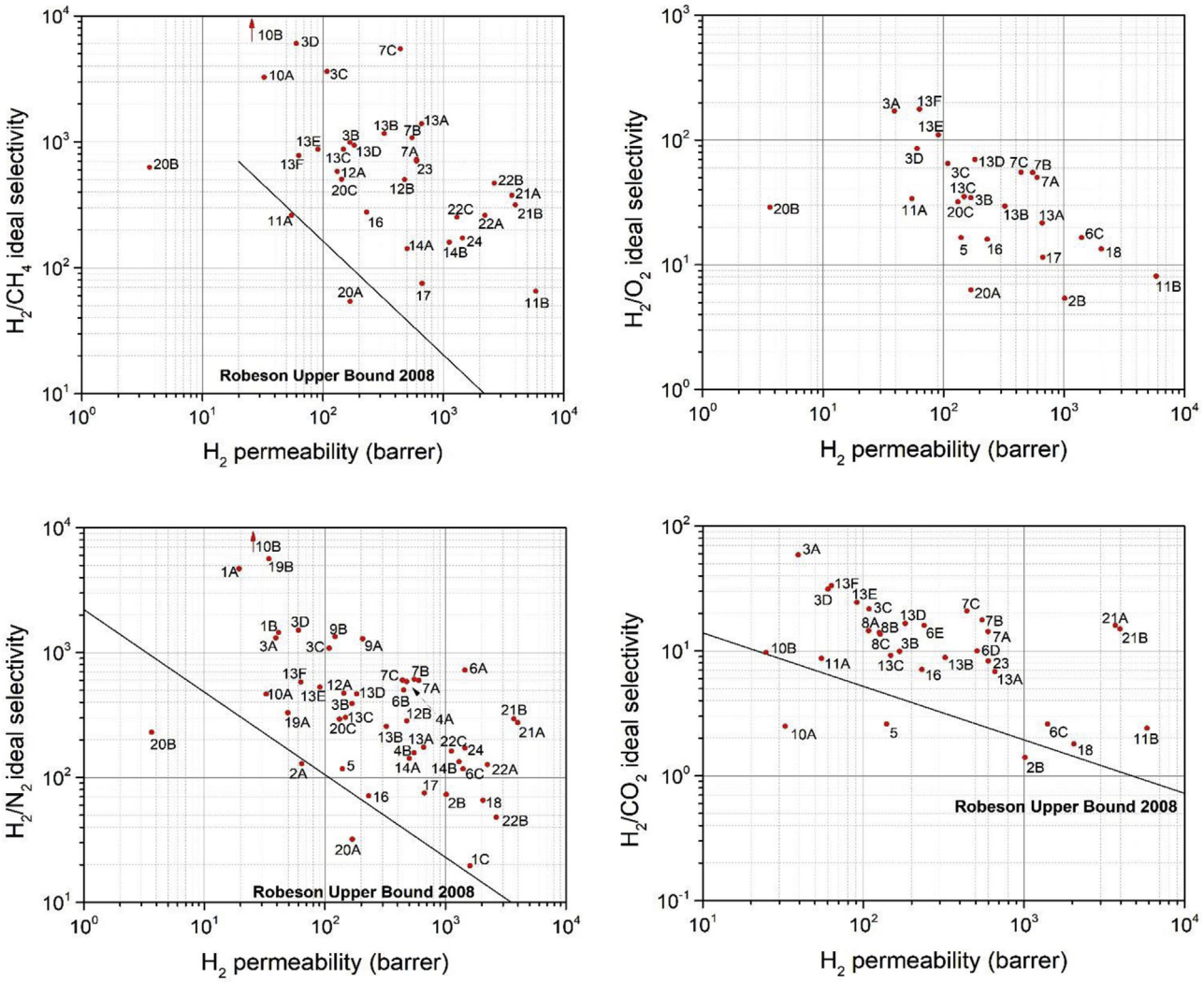

Fig. 1 – Robeson plots for the CMSMs referenced in this review.

Fig. 1 and Table S1). Favvas et al. [82] investigated the effect of the carbonization conditions of BTDA-TDI/MDI (P84) co-polyimide hollow fiber membranes, on the performance of the as-produced CMSMs. In general, an increase of the dwell time at 900 °C decreased the permeability of the membranes to all gases, due to a continuous densification process occurring at such temperature. However, the permeability decrease observed with CH_4 was much larger than with the other gases and therefore the H_2/CH_4 ideal selectivity increased abruptly with the dwell time, reaching a maximum value of 5500 in the case of the membrane CMS-900/60 (membranes 7A-7C in Fig. 1 and Table S1). Sá et al. [83] reported H_2/CO_2 selectivities in the range 13.6–14.5 in a study of the reaction of methanol steam reforming in a carbon membrane reactor in which CMSM supplied by Carbon Membranes Ltd were tested at 150 °C and 200 °C (membranes 8A-8C in Fig. 1 and Table S1). Very recently, Rodrigues et al. [84] reported the preparation of novel CMSMs with high separation performance and high stability in the presence of humidified streams, prepared from an ionic liquid-regenerated cellulose precursor. CMSMs carbonized at both temperatures of 550 and 600 °C displayed H_2/N_2 ideal selectivities well above the Robeson upper bound (membranes 9A, 9B in Fig. 1 and Table S1). In a different study, the same authors reported CMSM prepared from cellophane precursor films [85], carbonized at 550 °C and at 600 °C end temperatures, and exhibiting extremely high separation performance and stability even in the presence of humidity. CMSM 550 and CMSM 600 displayed quasi-linear humidity adsorption isotherms, which was assigned to the homogeneous hydrophilic character of the inner surface of the membranes. The CMSM 600 membrane displayed high ideal selectivities $H_2/N_2 > 25{,}000$, $H_2/CH_4 >> 25000$ and $H_2/O_2 = 44.5$ (membranes 10A, 10B in Fig. 1 and Table S1). The authors proposed the existence of two extreme sieving mechanisms: a gate sieving mechanism selective for spheroid gas species and a tubular sieving mechanism selective for linear gas species.

Effect of blending polymer precursors

Another strategy tested for improving the performance of CMSMs has consisted in the use of polymer blends as precursors. Zhou et al. [86] studied CMSMs prepared from a

Please cite this article as: Bernardo G et al., Recent advances in membrane technologies for hydrogen purification, International Journal of Hydrogen Energy, https://doi.org/10.1016/j.ijhydene.2019.06.162

precursor blend of a resol-type phenolic resin (PF) with a Novalak-type sulfonated phenolic resin (mass ratio 45:55). As an example, a membrane pyrolized at 500 °C displayed a permeability to H_2 of 5850 Barrer and an ideal H_2/CH_4 selectivity of 65 (membranes 11A and 11B in Fig. 1 and Table S1). CMSMs prepared from a precursor blend of phenol formaldehyde novolac resin (PFNR) and poly (ethylene glycol) (PEG) were studied by Zhang et al. [87]. PEG, due to its low thermal stability, acts as a pore-forming agent. CMSMs with different PEG:PFNR mass ratios (0.05, 0.1 and 0.15) and using PEGs with different molecular weights ($M_w = 2000$, 6000 and 10,000) were prepared and their gas separation performance tested. An increase of the PEG:PFNR ratio and of the PEG molecular weight, was shown to increase considerably the permeability of the CMSMs to gases without compromising significantly the corresponding H_2/CH_4 and H_2/N_2 selectivities (membranes 12A, 12B in Fig. 1 and Table S1). Hosseini et al. [88] prepared CMSMs using, as precursors, polymer blends of poly (benzimidazole) (PBI) with three other polymers, namely: Matrimid 5218, Torlon 4000T and P84. The different variables considered were the blend composition, the chemical modification with a cross-linking agent and the end temperature of pyrolysis. CMSMs derived from PBI/Matrimid exhibited better performance than from other blends and this was further improved by the addition of cross-linking agents. Increasing the pyrolysis temperature from 600 to 800 °C has also shown to lead to performance improvements. Overall, the authors prepared 6 different CMSMs derived from PBI/Matrimid blends (3 cross-linked and 3 non cross-linked) which all displayed H_2/CH_4, H_2/N_2 and H_2/CO_2 ideal selectivities well above the Robeson upper bound limit (membranes 13A-13F in Fig. 1 and Table S1). A polymer blend precursor, of the polymer poly (2,6-dimethyl-1,4-phenylene oxide) (PPO) and the polymer polyvinylpyrrolidone (PVP), was tested by Itta et al. [89] in the preparation of CMSMs on alumina support disks. The effects of PPO/PVP blend ratio and pyrolysis temperatures, on the separation performance, were both investigated and compared to the performance of pure PPO-based membranes. The two blend membranes carbonized at 700 °C, namely "PPO 10 PVP" and "PPO 15 PVP", both displayed H_2/N_2 and H_2/CH_4 separation performances above the Robeson upper bound limit (membranes 14A and 14B in Fig. 1 and Table S1). Sazali et al. [90] used, as precursor, a blend of P84 co-polyimide and nanocrystalline cellulose (NCC) as a strategy to nanostructure the membranes based on the unique rod-like nanostructure and low decomposition temperature of NCC. Different NCC loadings and different carbonization temperatures were tested. The best performing membranes were carbonized at 800 °C with 7% in mass of NCC additive and displayed an H_2/N_2 selectivity of 435 (membrane 15 in Fig. 1 and Table S1). Richter et al. [91] developed CMSMs, from a blend precursor of linear polyester molecules and styrene as cross-linking agent, supported inside asymmetric porous alumina tubes. The resulting CMSMs displayed a high permeability to H_2 of $P_{H2} \approx 231.2$ Barrer, and increasingly smaller permeabilities to other gases with increasingly higher molecular diameters, in agreement with a molecular sieving mechanism (membrane 16 in Fig. 1 and Table S1). Notably, the authors found that by an oxidative treatment in air, the transport mechanism of the membranes can be switched to a selective surface flow mechanism and the initially H_2 selective membranes are converted to membranes with CO_2 selectivity.

Effect of inorganic fillers and metal doping

The addition of inorganic fillers to the polymer precursor was also the subject of investigation by some authors. Tseng et al. [92] fabricated CMSMs, on α-alumina support disks, from a polyetherimide (PEI) precursor and mesoporous silica (SBA-15) as filler. Membranes with different mass fractions of SBA-15 (0, 0.5, 1.0, 3.0 and 5.0%) were produced and tested for their H_2 separation performance. The most promising membranes (SPEI-0.5) contained 0.5 wt% of SBA-15 and displayed a permeability to H_2 and H_2/N_2, H_2/CH_4 and H_2/O_2 selectivities significantly higher than the pristine membranes without SBA-15 (membrane 17 in Fig. 1 and Table S1). Teixeira et al. [93] prepared CMSMs from phenolic resin loaded with boehmite nanoparticles. An increase in the carbon/Al_2O_3 ratio was found to promote the formation of CMSMs with a more open porous structure and higher permeability, especially for the larger gas molecules. The best membranes for H_2 separation (M1) produced a selectivity for H_2/CO_2 very close to the Robeson upper bound and a selectivity for H_2/N_2 clearly above that limit (membrane 18 in Fig. 1 and Table S1).

Doping membranes with metal nanoparticles has been a strategy used by some authors to improve the hydrogen separation performance of CMSMs. Most often, platinum and palladium have been used as doping metals due to their high affinity towards hydrogen. Usually, the doping with metals is performed by dispersing metal compounds into the membrane precursor, that is before carbonization [94,95]. However, methods of doping after carbonization have also been developed [96]. Yoda et al. [94] used supercritical impregnation with CO_2 to prepare metal doped PI films as precursors for CMSMs. Platinum and palladium were tested as doping metals. After carbonization, the CMSMs doped with Pd displayed a more homogeneous metal nanoparticle distribution and a better separation performance than the corresponding Pt-doped membranes. Compared to the undoped membranes, the permeability of the Pd-doped membrane to N_2 decreased much more than the corresponding permeability to H_2 and as a result the Pd-doped CMSM displayed a H_2/N_2 selectivity of 5640 compared to the selectivity of 330 for an undoped CMSM (membranes 19A and 19B in Fig. 1 and Table S1). Kumakiri et al. [95] studied the effects of pyrolysis temperature and iron additives on the permeability and selectivity to H_2 of CMSM, prepared using organosolv-lignin and a phenol resin Bellpeal-S899 (BP) as precursors. Increasing the pyrolysis temperature, decreased the membrane permeability to H_2 but increased the selectivity to H_2 over other gases. The addition of 1.7 wt% of iron (III) acetate basic $(Fe(OH)(CH_3COO)_2)$, (FeAc) to the precursors, maintained the permeability to H_2 and simultaneously strongly increased the ideal selectivities H_2/N_2 and H_2/CH_4. The authors suggested that the iron additive distributes in the pores forming neck-like structures, that improve the H_2 selectivity without affecting its permeability. (membranes 20A-20C in Fig. 1 and Table S1). Wang et al. [96] doped CMSMs, prepared from a polyfurfuryl alcohol precursor, with palladium after their carbonization. Two different doping methods were tested, namely "impregnation-precipitation"

Please cite this article as: Bernardo G et al., Recent advances in membrane technologies for hydrogen purification, International Journal of Hydrogen Energy, https://doi.org/10.1016/j.ijhydene.2019.06.162

(IP) and "colloid impregnation" (CI). CMSMs doped with the IP method (Pd/C/Al_2O_3–IP membranes) displayed a more homogeneous distribution of Pd clusters and a better separation performance than the ones produced with the CI method (Pd/C/Al_2O_3–CI membranes). The effect of the palladium content on the separation performances of the Pd/C/Al_2O_3–IP membranes was further studied. The ideal selectivities of the gas pairs H_2/CH_4, H_2/N_2 and H_2/CO_2 increased with the Pd content attaining maximum values of 377, 295 and 16 respectively for a Pd/C = 0.4. The maximum permeability to H_2 (3970 Barrer) is attained for Pd/C = 0.1 (membranes 21A, 21B in Fig. 1 and Table S1).

Membrane-support interfacial effects

The interface between the selective membrane and the support in supported-CMSMs has been also the subject of some study. Wey et al. [97] studied how intermediate layers of mordenite framework inverted (MFI)-type zeolites, placed between the alumina support and the CMSM, affect the corresponding gas separation performance. Silica zeolite seeding and secondary growth of MFI layers were found to cause a decrease of the substrates pore sizes. Furthermore, the MFI intermediate layer increases the substrate polarity providing OH groups and consequently enhances and facilitates the CMSM layer formation. As an example, one of the best performing CMSMs with MFI interlayer displayed an H_2/CH_4 selectivity of 261 and a permeability to H_2 of 2224 Barrer (membranes 22A-22C in Fig. 1 and Table S1). More recently, Tseng et al. [98] studied the interfacial effect of planar titanium gel-modified alumina supports on the performance of supported CMSMs, prepared from a polyethyleneimine precursor. Bare Al_2O_3 supports were coated with different sol-gel intermediate layers of TiO_2 and later calcined at 400 °C, to produce supports with different quality. Later, a set of CMSMs were prepared on top of those different supports, using the same preparation conditions for all CMSMs. The support was shown to strongly affect the quality of the CMSM prepared on top. CMSMs prepared on TiO_2/Al_2O_3 composite supports displayed higher H_2/CH_4 and H_2/CO_2 selectivities than similar membranes prepared on bare Al_2O_3 supports. For example, although the membrane TiN4-3 displayed a permeability to H_2 of 601 Barrer, which is only slightly higher than from bare Al_2O_3 (537 Barrer), the corresponding ideal selectivities for the H_2/CH_4 and H_2/CO_2 gas pairs were considerably higher, namely 726 (198) and 8.3 (3.3), where values in parentheses are from the membrane prepared on bare Al_2O_3 (membrane 23 in Fig. 1 and Table S1).

Post-treatment effects

Post-treatments, *i.e.* after pyrolysis, have also been studied. Tseng et al. [99] modified the pore size and pore size distribution of alumina supported CMSMs, derived from PI and PEI precursors, by coating the surface of the previously carbonized CMSMs with a low viscosity poly (p-phenylene oxide) (PPO) casting solution, followed by a new carbonization at 600 °C. The PPO-modified membranes possessed a tighter submicrostructure, and compared with pristine CMSMs, displayed lower permeability to larger gases (N_2 and CH_4) but higher permeability to H_2. As a result, the ideal selectivities H_2/N_2 and H_2/CH_4 increased significantly after the PPO treatment. For example, for the PI-derived membranes the ideal selectivity H_2/N_2 increased from 17.1 (without PPO treatment) to 171.9 (with PPO treatment) and the ideal selectivity H_2/CH_4 increased from 8.8 to 172.4 (membrane 24 in Fig. 1 and Table S1).

Section conclusions

One important advantage of CMSM lies in the fact that they are particularly good for separating H_2 (kinetic diameter = 2.89 Å) from gas molecules with much larger kinetic diameters such as N_2 (3.64 Å), CH_4 (3.80 Å) and C_3H_8 (4.30 Å). The permeabilities of CMSM to H_2 are most often in the range 100–1000 Barrer, although values > 5000 Barrer have been reported [86]. The ideal selectivities for the separation of H_2/CH_4 and H_2/N_2 are most commonly in the ranges 100–2000, although values > 25000 have been recently reported for both gas pairs [85]. Although the selectivity of CMSM has been traditionally attributed to the so-called molecular sieving mechanism, two other different mechanisms have been recently proposed, namely: gate sieving and tubular sieving mechanisms. Other advantages of CMSM are that they are resistant to CO and sulphur poisoning and they are suitable for hydrogen separation at low temperatures. However, CMSMs also present several disadvantages. They are usually brittle, they exhibit rather small permeation fluxes and they perform poorly on the separation of H_2/CO_2 mixtures (best ideal selectivities < 60). Furthermore, these membranes still present considerable problems related to their stability when exposed to specific environments. In the presence of humidity, H_2O molecules tend to adsorb onto hydrophilic functional groups on the membrane's surface and then adsorbate-adsorbate hydrogen bonding interactions promote the adsorption of additional H_2O molecules originating small water clusters. Once formed, these clusters can block the pore network causing an abrupt decrease on the permeability of the membrane; this aging effect has so far seriously limited the commercialization of CMSMs.

Ionic liquid (IL)-Based membranes for CO_2/H_2 separation

General overview

As mentioned in the introduction, currently the main H_2 production method in the world consists in the SMR followed by the WGS reaction. Carbon dioxide is the main by-product of this unit operation and it must be removed from the H_2 stream, as the primary step in the H_2 purification. Presently, the most mature post-combustion CO_2 capture technology, with ~90% of the share market [100], is based on CO_2 chemical absorption by aqueous amine solutions. In a typical CO_2 absorption system, an amine solvent absorbs CO_2 at ~40 °C and releases the captured CO_2 upon heating at ~120 °C. The high temperature needed for regenerating the amine solvent makes the whole process very energy intensive [101,102]. Therefore, to enable CO_2 capture with as low energy

consumption as possible, there is an obvious need to develop more energy efficient solutions and membrane separation technology seems to be the most promising option.

Ionic liquid (IL) based membranes have emerged in the last 15 years as very promising candidates for CO_2 separation from gas streams (CO_2/N_2, CO_2/CH_4, CO_2/H_2) and have been the topic of several reviews [100,103–111]. Ionic liquids (ILs) are salts [112,113], normally either liquids at room temperature or solids with melting temperatures below 100 °C, with a chemical structure formed by an organic cation and an organic or inorganic anion. Compared to traditional organic solvents, ILs have several advantages such as negligible vapour pressure, non-flammability and a set of additional physicochemical properties that can be tailored through a different combination of cations and anions.

One very important characteristic of ILs that makes them particularly suitable for the separation of CO_2/H_2 mixtures is the fact that the solubility of CO_2 in ILs is higher than the corresponding solubility of H_2, with a consequent remarkable CO_2 selectivity over H_2 [114]. Among ILs, anions having fluoroalkyl groups were found to possess higher CO_2 sorption, which increases as the quantity of fluoroalkyl groups increases. For example, the bis(trifluoromethylsulfonyl)imide [Tf2N] anion has a very high CO_2 affinity. Interestingly, the sorption of H_2 in ILs tends to increase with temperature, contrary to the sorption of CO_2 [114]. As a consequence, for a pure sorption-diffusion mechanism, the CO_2/H_2 selectivity of IL-based membranes decreases with temperature. However, if a facilitated transport mechanism involving CO_2 complexation with a carrier is present, then the CO_2/H_2 selectivity may increase with temperature.

Different types of membranes containing ILs have been reported over time, including: i) supported IL membranes (SILMs); ii) polymer-IL composite membranes; iii) polymer-IL gel membranes; iv) polymerized ionic liquid or poly (ionic liquid) membranes (PILM) and v) PILM-ILs composite membranes.

SILMs are intrinsically microporous membranes prepared by impregnating the pores of a porous support (polymeric, ceramic, etc.) with ILs, which are immobilized by capillary forces inside the pores. SILMs cannot withstand practical pressure drops in gas separation because they suffer IL leaching over time which severely degrades the membrane's performance [115].

Polymer-IL composite membranes are usually produced by solvent casting polymer-IL blends from a solution, and allowing the film to dry. These membranes usually display a microphase-separated structure being the IL entrapped between the plasticized polymer chains.

Polymer-IL gel membranes are usually produced also by solvent casting polymer-IL blends from a solution, but in this case the polymer and IL form physical gels due to hydrogen bonding interactions. Polymer-IL gel membranes usually suffer from poor mechanical stability and also from poor thermal stability (operation close to room temperature) that is limited by the gelation temperature (*i.e.* the temperature at which the gel reversibly becomes a fluid).

PILM are produced by polymerizing or crosslinking either IL monomers or polymer chains containing IL-based functional groups, forming a macromolecular architecture. PILM combine the advantages of polymers, namely improvement of the mechanical stability, and the advantages of ILs, namely the ability to tailor the chemical and physical properties of the membrane. PILM-ILs composite membranes are produced by blending PILM with ILs. These composite membranes are very stable and can withstand large pressure gradients without leaching because the Coulombic attraction between PILM and free ILs are much stronger than those between ILs and conventional uncharged polymers and far outweighs the external pressure [116].

The transport of light gases in Ionic Liquid (IL)-Based Membranes follows the sorption-diffusion mechanism, where permeability (P) is equal to the product of gas diffusivity (D) and sorption (S) in the polymer, *i.e.* $P = D{\cdot}S$. It then follows that the membrane ideal permeability selectivity ($\alpha_{i/j}$) is the ratio of permeabilities of two permeating species (i and j). The permselectivity can also be represented as the product of diffusivity selectivity and sorption selectivity [117].

The sorption-diffusion mechanism in ionic liquid-based membranes can be facilitated by a CO_2-selective transport mechanism. This so called CO_2-selective facilitated transport utilizes reactions between CO_2 and CO_2 carriers to enhance the transport of CO_2 through the membrane, resulting in a significantly improved permeability and selectivity of the membrane to CO_2 [118,119].

As the permeability to CO_2 in ionic liquid-based membranes is usually higher than the permeability to H_2, these are CO_2-selective membranes that can permeate CO_2, and retain H_2 and other impurities (CH_4, CO), producing high-pressure H_2 (retentate side) and low-pressure CO_2 (permeate side).

In terms of economic viability, ILs are still mostly used and produced at the lab scale which is very far from the industrial scale in terms of costs. Although there are several vendors that provide ILs for various purposes, their prices are still, in general, 100–1000 times more expensive compared to the conventional solvents [112]. IL prices are expected to drop with their industrial production but, due to the complexity involved in their synthesis and purification, they should end *ca.* 10x the price of conventional solvents. Although the economic potential of ionic liquids as solvents for general CO_2 capture has been evaluated [120], no studies are known on the economic viability of ionic-liquid based membranes for H_2 purification.

Several review articles dealing with IL-based membranes for gas separation have been previously published, as mentioned and referenced above, but these were not specifically focused on CO_2/H_2 separations. In fact, the majority of gas separation studies involving ionic-liquid based membranes have been focused on the separation of CO_2/N_2 and CO_2/CH_4 gas mixtures, while the separation of CO_2/H_2 mixtures has been much less reported. This review section presents and discusses the most relevant studies in the separation of CO_2/H_2 mixtures using IL-based membranes. Fig. 2 and Table S2 in supporting information summarize the most relevant separation performances (permeability to CO_2; CO_2/H_2 selectivity) reported in the literature and based on IL-based membranes.

Although, as indicated in Table S2 in supporting information, IL-based membranes are typically used either at room temperature or at temperatures slightly above room

Please cite this article as: Bernardo G et al., Recent advances in membrane technologies for hydrogen purification, International Journal of Hydrogen Energy, https://doi.org/10.1016/j.ijhydene.2019.06.162

temperature, they can also be used at higher temperatures. For example: the operation of SILMs, based on polymeric supports, at temperatures up to 175 °C has been reported [121] and at higher temperatures (200 °C) using ceramic supports [122]; similarly, polymer-IL composite membranes can also be used at temperatures as high as 200 °C [123].

SILMs for CO_2/H_2 separation

Initial interest in the use of ILs within gas separation membranes focused on supported ionic liquid membranes (SILM). Myers et al. [121] prepared a SILM, with facilitated transport, consisting of an amine-functionalized ionic liquid [$H_2NC_3H_6$-mim][Tf_2N] encapsulated in a cross-linked Nylon 66 polymeric support. Permeability measurements were made up to 175 °C, without any loss of stability of the membrane. The CO_2/H_2 selectivity increases with temperature reaching a maximum of ~20 at 85 °C and then decreases at higher temperatures (membranes 1A and 1B in Fig. 2 and Table S2). SILMs, for separation and enrichment of H_2, supported in a polyvinylidene fluoride (PVDF) hydrophobic membrane with pore size of 0.22 μm and based on ionic liquids containing the 1-n-alkyl-3-methylimidazolium cation with different alkyl chain lengths and different anions, were prepared and studied by Neves et al. [124]. The CO_2/H_2 selectivity was found to be more dependent on the presence of different anions than on the chain length of the IL cation: the obtained CO_2/H_2 selectivities varied between 5 and 11 (membranes 2A-2D in Fig. 2 and Table S2). A supporting PVDF membrane, with pore size of 0.22 μm and porosity of 75%, was also used by Cserjesi et al. [125] in the preparation of SILMs with eight different ionic liquids. After the permeation of CO_2, the permeability to H_2 of most SILMs increased while their CO_2/H_2 selectivity decreased. This unfavourable effect of CO_2 on the separation properties was attributed to a likely plasticization of the supporting polymer membrane by CO_2 (membranes 3A-3H in Fig. 2 and Table S2). More recently, Liu et al. [126] prepared four PVDF-based SILMs with pore size of 0.10 μm and using four different ionic liquids, namely: [BMIM][DCA], [BMIM][AC], [BMIM][TfO] and [BMIM][NTf_2]. At the testing temperature of 30 °C, the SILM with [BMIM][NTf_2] showed the best separation performance for CO_2/H_2 with a permeability to CO_2 of 3883 Barrer and an ideal CO_2/H_2 selectivity of 14.2 (membranes 4A-4D in Fig. 2 and Table S2). Other studies have also reported the preparation of SILMs and study of their performance for CO_2/H_2 separations, but with less interesting performances [127,128] (membranes 5A-5D, 6A, 6B in Fig. 2 and Table S2).

Polymer-IL composite membranes for CO_2/H_2 separation

Chen et al. [129] prepared polymer-IL composite membranes based on PVDF and the ionic liquid [EMIM][$B(CN)_4$] and studied the effect of composition (PVDF:IL ratios of 2:1, 1:1 and 1:2) on the separation performance of the membranes. Both the permeability to CO_2 and H_2 and the CO_2/H_2 ideal selectivity were observed to increase with the ionic liquid content. The best performing membranes, with a PVDF:IL ratio of 1:2, showed a high permeability to CO_2 of 1778 Barrer with a CO_2/H_2 selectivity of 12.9 (membranes 7A-7C in Fig. 2 and Table S2). These 1:2 membranes were also shown to be the most heterogeneous containing larger phase segregated domains and larger fractional free volumes (FFV), as revealed respectively by polarized light microscopy and positron annihilation spectroscopy. All the membranes proved to be stable under *trans*-membrane pressure gradients up to 5 atm. Bernardo et al. [130] studied composite membranes based on Pebax1657, a copolymer with 60 wt% of poly (ethylene oxide) (PEO) and 40 wt% of polyamide-6 (PA-6), and the IL [BMIM][CF_3SO_3]. Differential scanning calorimetry (DSC) measurements suggests a high compatibility between the polymer and the IL. The membranes with the best CO_2/H_2 separation performance had 60 wt% [BMIM][CF_3SO_3], displayed a permeability to CO_2 of 200 Barrer and an ideal CO_2/H_2 selectivity of 8.3 (membrane 8 in Fig. 2 and Table S2). Composite membranes based on PI and the IL [BMIM][Tf2N] were prepared and studied by Kanehashi et al. [131] who investigated the effect of the IL content, from 0 up to 81 wt%, on the membrane's separation performances. The permeabilities to H_2 and CO_2 were observed to decrease with IL content up to 35 wt%, then remained stable up to 51 wt % IL and finally increased with higher IL contents up to 81 wt%. This transition was attributed to a morphological transition, observed using scanning electron microscopy (SEM) and corroborated by DSC measurements, from a homogeneous system at lower IL loadings to a phase-separated system at higher IL loadings. The composite membranes with higher IL content (81 wt%) showed the best CO_2/H_2 separation performance (membranes 9A, 9B in Fig. 2 and Table S2). Rabiee et al. [132] prepared polymer-IL composite membranes based on the copolymer Pebax1657 and the ionic liquid [EMIM][BF_4] and studied the effect of ionic liquid content (copolymer:IL mass ratios varying from 5:1 to 1:1) on the morphology and gas separation performance of the membranes. The membranes with the best CO_2/H_2 separation performance were those containing the highest ratio of IL (copolymer:IL ratio of 1:1) and displayed a permeability to CO_2 of 505.1 Barrer and an ideal CO_2/H_2 selectivity of 19.9 (membranes 10A-10C in Fig. 2 and Table S2). Based on DSC measurements, the authors concluded that the crystallinity of the membranes decreases with the IL content and therefore the best performing membranes were also less crystalline and contained a higher FFV than the other membranes.

Polymer-IL gel membranes for CO_2/H_2 separation

Jansen et al. [133,134] prepared polymer-IL gel membranes based on the copolymer poly (vinylidene fluoride-co-hexafluoropropylene) (p (VDF-HFP)) and on the ionic liquid [EMIM][TFSI]. Although the permeabilities to both CO_2 and H_2 increased with the IL content in the membrane, the permeability to CO_2 increases much faster than the permeability to H_2 due to its much higher solubility and therefore the CO_2/H_2 selectivity increases. The best performing membranes for CO_2/H_2 separation had an IL content of 80 wt% and displayed a permeability to CO_2 of 533 Barrer and a CO_2/H_2 ideal selectivity of 12.3 (membrane 11 in Fig. 2 and Table S2). Wide-angle X-ray diffraction and DSC measurements suggest that the presence of IL favours the formation of different copolymer polymorphs (γ instead of α). In a similar work with p (VDF-HFP) but using ionic liquid mixtures [135], lower CO_2/H_2 separation performances were reported by the same authors (membranes 12 in

Please cite this article as: Bernardo G et al., Recent advances in membrane technologies for hydrogen purification, International Journal of Hydrogen Energy, https://doi.org/10.1016/j.ijhydene.2019.06.162

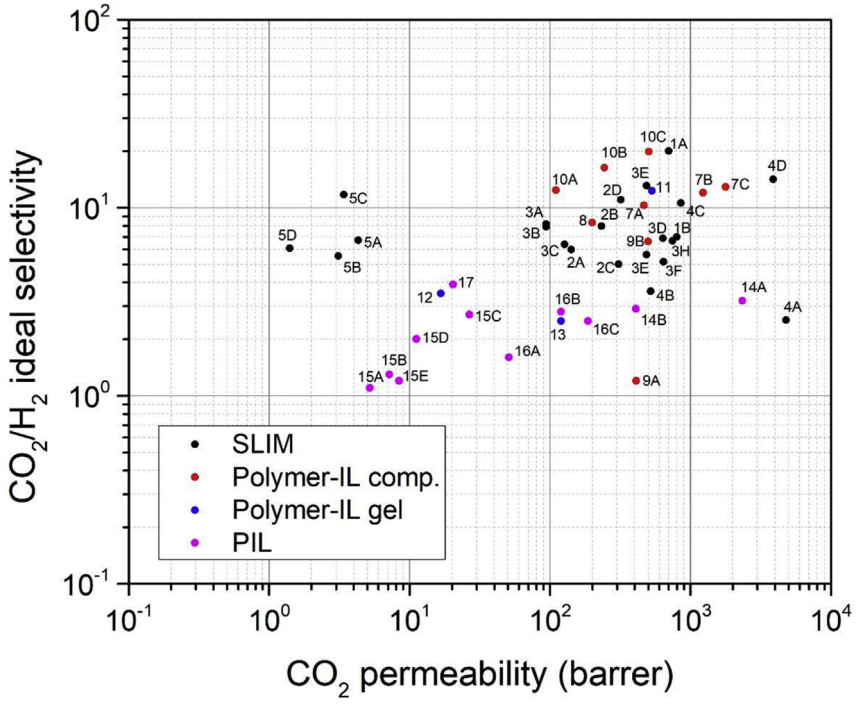

Fig. 2 – Robeson diagram for the gas pair CO_2/H_2 indicating the experimental points of the present review.

Fig. 2 and Table S2). Couto et al. [136] prepared, on cellulose supports, polymer-IL gel membranes based on gelatine and the ionic liquid [BMIM][DCA] which displayed a permeability to CO_2 of 120 Barrer and a CO_2/H_2 ideal selectivity of 2.5 (membrane 13 in Fig. 2 and Table S2).

PILM and PILM-IL membranes for CO_2/H_2 separation

Gas separation membranes made from PILs were first reported in 2007 by Bara et al. [137] with the aim of solving the problem of IL leaching that is usually observed in SILMs. However, in this initial work the permeability to H_2 was not studied. In fact, at this point it is worth mentioning that a large part of the gas separation studies reported in the literature using PILM are focused on the gas pairs CO_2/N_2 and CO_2/CH_4 and do not consider CO_2/H_2. In this section, we describe the few studies that have addressed the CO_2/H_2 system.

Wiesenauer et al. [138] prepared PILM based on triblock copolymer systems containing an hydrophobic block (block A), an imidazolium ionic liquid (IL)-based block (block B) and an uncharged hydrophilic block (block C) and exhibiting an ordered nanophase-separated morphology. The overall block length ratio of the triblock copolymer was set to (1:1:1), with the total polymer length close to 60 repeating units and, therefore, each block segment had ~ 20 monomer repeated units. PILM, coated on top of a PAN support, were tested for their CO_2/H_2 separation performance and the best performing membranes (with a block copolymer sequence ABC) displayed an impressive permeability to CO_2 of 2340 Barrer and an ideal CO_2/H_2 selectivity of 3.2 (membranes 14A, 14B in Fig. 2 and Table S2). Five different composite PILM-IL membranes were also prepared by Zarca et al. [139], via radical photopolymerization of the polymerizable IL [C_4vim][Tf_2N] and the non-polymerizable IL [C_4mim][Cl] in the presence of CuCl. These membranes were prepared, using different relative amounts of [C_4vim][Tf_2N], [C_4mim][Cl] and CuCl, including a reference poly ([C_4vim][Tf_2N]) membrane prepared from the pure polymerizable IL. The permeability results showed that increasing the relative amount of non-polymerizable IL enhanced the permeabilities to both CO_2 and H_2, as well as the CO_2/H_2 selectivities, relative to those obtained in the pristine poly ([C_4vim][Tf_2N]). On the other hand, although the addition of CuCl proved beneficial for H_2/N_2 separations, it decreased both the permeability to CO_2 as well as the CO_2/H_2 selectivity. Therefore, the best performing membranes for CO_2/H_2 separation, with a permeability to CO_2 of 26.7 Barrer and a CO_2/H_2 selectivity of 2.7, contained no CuCl and were prepared with 75% molar of polymerizable [C_4vim][Tf_2N] and 25% molar of the non-polymerizable [C_4mim][Cl] (membranes 15A-15E in Fig. 2 and Table S2). Cowan et al. [140] reported the preparation and study of free-standing PILM based on the free radical polymerization of a homologous series of (tri-n-alkyl)vinylbenzylphosphonium monomers with the bis(trifluoromethylsulfonyl) imide anion: [P_{nnnVB}][Tf_2N]. The resulting PILM (*i.e.* poly ([P_{nnnVB}][Tf_2N]) where $n = 4, 6, 8$) were characterized for their single-gas transport properties. The gas permeability to CO_2 was found to increase approximately linearly with increasing alkyl chain length on the phosphonium group (from $n = 4$ to $n = 8$) reaching the value 186 Barrer with the octyl chain ($n = 8$). However, the ideal CO_2/H_2 selectivity attained its maximum value (2.8) with the hexyl chain ($n = 6$) on the phosphonium group (membranes 16A-16C in Fig. 2 and Table S2). In another study, PI with imidazolium cations directly located within the polymer backbone were synthesized by Mittenthal et al. [141]. The produced ionic PI, in the form of a fine powder, was then extruded into pellets and

finally melt pressed into defect-free PILM films with a thickness of ~90 μm. These films were then soaked with the ionic liquid [C4mim][Tf2N], producing PILM-IL that were tested for the gas separation performance, together with the neat PILM. The neat PILM displayed very low permeability to both CO_2 (~0.9 Barrer) and H_2 (~1.6 Barrer). By contrast, the PILM-IL showed a great improvement in the respective permeabilities to CO_2 and H_2, which increased to 20.4 Barrer and 5.2 Barrer respectively (membrane 17 in Fig. 2 and Table S2). This increase in permeability was due to an increase in diffusivity, as the sorption of each gas was similar in both membranes types. Furthermore, this ionic PI PILM-IL composite proved mechanically robust and stable against leaching, as the IL could not be squeezed out of the composite under applied pressure. The cross-section of the neat PILM is dense and largely homogeneous, while that of the PILM-IL composite shows morphological changes throughout the bulk. Although the performances of these first ionic PI + IL composite membranes fall clearly short of the industrial requirements, there are thousands of different ionic PI structures that can be produced, due to the possible combinations of precursors. Therefore, this work seems to have opened new exciting directions to the large-scale melt processed industrial production of high-performance gas separation membranes for CO_2/H_2 mixtures.

Section conclusions

In conclusion, for CO_2/H_2 membrane separations to become economically competitive with the current industrial amine-based processes, both high permeability and selectivity to CO_2 are required. Although the CO_2/H_2 separation performances of PILM are still far from the industrial requirements, PILM are a very recent technology and the potential for their optimization and improvement is very high. By synthesizing new PILM and blending in free ILs with high permeability and selectivity, PILM-IL composites have the potential to achieve excellent separation performances. These, associated with the large reduction in the price of ILs that is expected to occur with their large scale production, have the potential to bring these type of membranes to commercialization.

Palladium based membranes

General overview

The discovery of the hydrogen capability to permeate through bulk metals dates from 1863 [142] and the first use of palladium membranes to separate hydrogen from gas mixtures dates from 1866 [143]. However, only a century later, in the 1960s, this topic has started attracting an increasing interest from the scientific community [144] which has intensified in recent years [145,146] due to the increased awareness of the important role that hydrogen will likely play soon as an important energy vector.

The mechanism of hydrogen transport through dense metal membranes has been extensively studied and it is now well established; it occurs via a sorption–diffusion mechanism. The steps involved in hydrogen permeation from a high to a low partial pressure gas region are the following: i) dissociative adsorption of H_2 on the gas-metal interface; ii) sorption of the atomic hydrogen into the bulk metal; iii) diffusion of atomic hydrogen through the bulk metal membrane; iv) re-combination of atomic hydrogen to form hydrogen molecules at the interface metal/gas permeate; v) desorption of molecular hydrogen.

The hydrogen permeation flux (J_{H2}) through a dense metal membrane (mol·m^{-2}·s^{-1}), derived combining Fick and Sieverts' laws, can be expressed as:

$$J_{H_2} = \frac{P_{H_2}}{\delta}\left(\left(p_{H_2}^{ret}\right)^n - \left(p_{H_2}^{perm}\right)^n\right) \quad (1)$$

where P_{H2} is the permeability to hydrogen (mol m m^{-2} s^{-1} Pa$^{-1/2}$), δ the membrane thickness (m), $p_{H2,ret}$ and $p_{H2,perm}$ the hydrogen partial pressures at the retentate and permeate sides respectively and the exponential factor n is the pressure exponent (ranging from 0.5 to 1, n = 0.5 when the rate limiting step is the bulk diffusion through the metal layer and n = 1 when the surface reactions are the rate limiting step). The permeability to hydrogen is equal to the product of the diffusion and sorption coefficients, $P = D{\cdot}S$.

Metals like niobium (Nb), vanadium (V) and tantalum (Ta), have higher hydrogen permeation flux than Pd, in the temperature range between 0 and 700 °C. However, contrary to what happens in palladium surfaces, in most metal surfaces the dissociative adsorption of H_2 has an activation barrier and therefore requires an energy input which may involve the application of high hydrogen pressures or elevated temperatures. On palladium the dissociative adsorption of H_2 molecules requires little or no activation energy [147]. Compared to other metals, palladium has a superior catalytic activity to dissociation of molecular hydrogen and a high permeability to atomic hydrogen. Furthermore, its inherent selectivity for hydrogen, allowing hydrogen permeation while, at the same time, avoiding the permeation of other molecules, confers to Pd-based membranes virtually infinite selectivities and allow the production of ultra-pure hydrogen at 99.99999% purity. For these reasons, palladium is considered the most suitable metal for H_2 purification membranes and membranes based on Pd and Pd-alloys have completely dominated the field in the last decades.

Depending on their structure, palladium-based membranes can be classified either as unsupported (free-standing) membranes or as supported membranes. Unsupported membranes were popular from the early stages of palladium membrane research until the late 1980s. A major problem of unsupported palladium membranes is that they need to be thicker than ~20–30 μm to guarantee their mechanical stability, and as a consequence they display low hydrogen flux and are very expensive. The use of these membranes has largely fallen into disuse except for applications requiring H_2 with extremely high purity.

Supported palladium membranes are usually prepared by depositing a thin Pd layer over porous supports, usually either ceramic or metallic, which confer to the system the necessary mechanical stability. Current state-of-the-art research is focused on supported membranes. The great advantage of porous supports is that they allow to reduce metal membrane thickness below 1 μm, with a consequent very large increase

Please cite this article as: Bernardo G et al., Recent advances in membrane technologies for hydrogen purification, International Journal of Hydrogen Energy, https://doi.org/10.1016/j.ijhydene.2019.06.162

in hydrogen flux and a large decrease in price, without compromising the structural integrity of the membrane. However, supported membranes may also suffer from some problems such as poor adhesion between the membrane and the support [148] and element migration from the support to the membrane films at high temperatures [149] that can degrade the permeability to hydrogen and ultimately cause membrane failure. Furthermore, the minimum thickness of the metal membrane required to achieve a continuous uniform film is crucially dependent on the smoothness of the support – rough surfaces require thicker films than smooth surfaces [150].

Despite the advantages of palladium over other metals, pure palladium membranes also have their associated problems. The most important of these is the so-called "hydrogen embrittlement" phenomenon. At temperatures below 300 °C and pressure below 2.0 MPa, the pure Pd suffers a $\alpha \rightarrow \beta$ lattice phase transition, resulting in a ~10% volume expansion, which induces internal stress in the lattice structure causing the pure palladium membrane to become brittle. Therefore, Pd membranes are not suitable for use at low temperatures. Another major problem associated with pure Pd membranes is their unsatisfactory chemical stability [151] due to their high susceptibility to poisoning by contaminants such as carbon monoxide (CO) [152–156], H_2O steam [152,153] and sulphur compounds [157–161]. These contaminant molecules adsorb on the palladium surface blocking potential hydrogen adsorption sites and therefore reduce considerably the permeability to H_2. These critical issues of chemical and thermal stability remain as the main obstacles for the commercialization of these type of membranes.

Several techno-economic assessments of the use of palladium membranes for H_2 purification, especially when incorporated in membrane reactors, have been reported in the literature [162–164]. In general, these support the economic viability of the use of these membranes especially when used in low volume production. For example, O'Donnell et al. [164] compared the costs of H_2 production in a fluidized bed membrane reactor (FBMR) equipped with Pd membrane and the costs of H_2 production in a benchmark SMR system with PSA. The results show that FBMR with palladium membrane has the greatest price benefits for volume productions <1000 kg/day and these benefits taper off at production volumes >5000 kg/day.

There have been in recent years a large number of review articles in the topic of palladium based membranes for hydrogen purification [165–172] and therefore in this review section we focus only on some very recent and more relevant studies. This very recent research has mostly focused on the improvement of the chemical and thermal stability as well as on the improvement of the permeability and cost efficiency of the membranes.

Following a trend that comes from many years ago, to overcome poisoning problems and the hydrogen embrittlement phenomenon while simultaneously maximize the permeability to hydrogen, much of the latest research has been focused on the development and optimization of binary and ternary Pd-based alloy membranes. A much newer research direction to improve the chemical resistance consists in the deposition of protective zeolite or ceramic layers on top of the palladium-based membranes. A third research topic consists in the production and optimization of cost-effective ultra-thin Pd-based membranes. The various types of recent palladium-based membranes are reviewed below and their performances summarized in Table 1.

Palladium alloying

Alloying of palladium with transition metals has been known for a long time to improve the performance as well as the chemical and thermal stability of the palladium-based membranes [168,171,173]. At present, most of the metal-based hydrogen separation membranes are based on Pd–Ag and Pd–Cu alloys and the study of Pd-alloys for H_2 separation continues receiving a very significant scientific interest. Lee et al. [174], aiming the separation of hydrogen from chlorosilane gases in silicon-based industries, demonstrated that the addition of Ru to Pd membranes (with Ru content between 1 and 10%) increases the resistance to hydrogen embrittlement as well as the chemical resistance to HCl and $SiHCl_3$ impurities. However, the observed hydrogen permeation flux was rather low (1.8 $m^3\ m^{-2}\ h^{-1}$). Melendez et al. [175] observed that the addition of Au to the Pd–Ag membranes increases their resistance to H_2S poisoning. In fact, whereas Pd–Ag–Au membranes resisted 12.5 h of H_2S exposure showing recovery rates of up to 85%, the hydrogen flux of Pd–Ag membranes decreased below detectable values. H_2S was shown to induce the formation of polyhedral crystals on the membrane's surface, being this phenomenon much less pronounced in the Pd–Ag–Au alloys. Infrared-reflection absorption spectroscopy (IRAS) in the temperature range 100–260 °C was used by O'Brien et al. [156] to study the CO poisoning mechanism in a 25 μm-thick $Pd_{47}Cu_{53}$ (molar fraction) membrane. CO has a stronger interaction with Pd sites than with Cu sites and was observed to adsorb only on Pd sites, blocking H_2 dissociation on those sites. Therefore, the PdCu alloy is more resistant to CO poisoning than the pure Pd. PdCu, PdAu, and PdCuAu alloy membranes, supported on porous ceramic tubes, were studied by Jia et al. [176], in the temperature range 500 °C–650 °C. Although the membranes containing Au showed higher hydrogen permeation (J_{H2}), the PdCu membranes demonstrated to be much more temperature stable than the PdAu, and PdCuAu membranes. Fontana et al. [177] studied the poisoning effect of CO, CO_2 and H_2S, on the hydrogen permeance of binary PdAu and ternary PdAgAu alloy membranes, prepared by the electroless plating technique. Under CO containing streams, the PdAgAu ternary alloy membranes showed a lower decrease of the permeance to hydrogen than the binary PdAu alloy. By contrast, in the presence of CO_2, the ternary alloy showed a higher permeance decrease with a complete hydrogen recovery after removing CO_2 from the stream. In the presence of H_2S, both PdAu and PdAgAu alloy membranes suffered high permeance decrease and after H_2S removal the hydrogen permeance recovery was only partial.

Intermediate support layers

The use of intermediate oxide support layers has been explored by some authors. In 2015, Alique et al. [178] demonstrated the use of a laboratory reactor equipped with a Pd

Please cite this article as: Bernardo G et al., Recent advances in membrane technologies for hydrogen purification, International Journal of Hydrogen Energy, https://doi.org/10.1016/j.ijhydene.2019.06.162

membrane (10 μm) deposited by ELP on top of an intermediate support layer of Fe–Cr oxides, on a cylindrical porous stainless steel (PSS) support, for performing the WGS reaction. CO conversion was found to be higher when using the Pd/Fe–Cr oxides/PSS membrane to separate H_2. Very recently, the same authors reported [179] the incorporation of a ceria (cerium (IV) oxide) intermediate layer between the oxidized PSS support and the Pd membrane, deposited by ELP, producing Pd (~15 μm)/CeO_2/PSS composite membranes. CeO_2 was shown to reduce both the average pore size and the external roughness of the oxidized PSS support tubes. This composite membrane exhibited a hydrogen permeance of 5.4×10^{-4} mol m^{-2} s^{-1}·$Pa^{-1/2}$ at 400 °C and an ideal H_2/N_2 perm-selectivity ≥ 10000. Goldbach et al. [180] observed that a composite Pd/ceramic/Pd membrane, with Pd layers on both sides of a porous ceramic tube, exhibits similar permeability to H_2 (1.01×10^{-8} mol m^{-1} s^{-1}·$Pa^{-1/2}$ at 500 °C) but its H_2/N_2 selectivity (18033) is enhanced by an order of magnitude at 500 °C and $\Delta P = 500$ kPa compared to that of a similar Pd/ceramic membrane containing a Pd layer only on the outside of the ceramic tube.

Protective layers

A new research strategy to improve the chemical resistance of the membranes and decrease poisoning, initiated recently [181,182], consists in depositing porous protective layers (zeolite, ceramic) on the surface of the palladium membrane. This strategy is based on the simple principle that the impurity gases with a kinetic diameter larger than the zeolite or ceramic pore size are prevented from coming in direct contact with the Pd composite membrane. Guo et al. [183] reported a novel assembly method, combined with secondary growth technique, for growing a continuous and compact TS-1 zeolite film on the outer surface of a palladium membrane. The zeolite film effectively protected the Pd-based membrane from contamination, and greatly improved its operational stability. A similar idea was followed by Yu et al. [184] who synthesized a zeolite protective layer on the surface of a Pd composite membrane. This protective layer proved very effective at increasing the chemical stability of the Pd membrane. In a related work [185] the same authors suggested the use of a similar strategy for repairing defects in palladium-based membranes. Aiming to protect the surface of thin (~1 μm) PdAg supported membranes, from particles in a fluidized bed membrane reactor, Arratibel et al. [186,187] deposited a thin (~0.6 μm) mesoporous ceramic protecting layer on top of the Pd–Ag membrane, by a dip-coating technique. H_2 permeance and H_2/N_2 perm-selectivity, measured at 400 °C and 1 bar of transmembrane pressure difference, reached outstanding values of 5×10^{-6} mol m^{-2} s^{-1} Pa^{-1} and >25000, respectively [186]. These so-called double-skin membranes largely enhanced the stability of the performance of membranes under fluidization conditions, paving the way for their application in fluidized bed membrane reactors [187].

Ultra-thin membranes

An enormous increase in the world supply of palladium would be needed to satisfy the needs for producing Pd membranes for large-scale industrial purification of hydrogen [188]. Aiming to increase the cost-effectiveness of Pd membranes, as well as their hydrogen permeation flux, some recent research has been focused on the production and characterization of ultra-thin membranes. Tanaka's group [189] prepared ultra-thin (~1 μm thick) composite Pd–Ag membranes, on top of alumina tubes with an outer ZrO_2 layer, by a combination of PVD magnetron sputtering and electroless plating (ELP) technique. The membranes exhibited very high permeance to H_2 (8×10^{-6} mol m^{-2} s^{-1}·Pa^{-1} at 400 °C and 100 kPa) and a good perm-selectivity ($H_2/N_2 \approx 500$ at 400 °C). The first PVD layer was observed to copy the surface profile of the ZrO_2 support while the second ELP layer closed the pores increasing considerably the permselectivity. The same authors [190] reported thin-film (4–5 μm thick) Pd–Ag supported membranes, prepared by simultaneous Pd–Ag ELP deposition, containing a ceramic interdiffusion barrier layer between the metallic support and the Pd–Ag layer. These membranes exhibited a lower permeance to H_2 (1×10^{-6} mol m^{-2} s^{-1}·Pa^{-1} at 400 °C and 100 kPa) but extremely high H_2/N_2 permselectivities (>200,000). In another work by the same group [191], ultra-thin Pd–Ag supported membranes with different thickness (ranging from 0.46 to 1.29 μm) were prepared by ELP onto asymmetric tubular porous alumina supports. Although the 0.46 μm thick membrane showed an extremely high permeance to H_2 of 1.56×10^{-5} mol m^{-2} s^{-1} Pa^{-1}, at 400 °C under 1 bar of transmembrane pressure difference, its H_2/N_2 ideal perm-selectivity was quite low (~50). Increasing the thickness to 1.29 μm, the permeance to H_2 decreased to ~9.0×10^{-6} mol m^{-2} s^{-1} Pa^{-1} but the H_2/N_2 ideal perm-selectivity increased to 3300. The 1.29 μm membrane showed stable H_2 permeance and H_2/N_2 perm-selectivity in 100 h test. Kim et al. [192,193] deposited ultra-thin (<<1 μm) uniform Pd films on highly-hydrogen-permeable polymeric PBI-HFA supports by ELP. Some of the best performing membranes [192], with a thickness of 273 nm, exhibited a permeability to H_2 of 276 Barrer and ideal selectivities H_2/N_2, H_2/CO and H_2/CO_2 of 46, ∞ and 65, respectively. Other membranes [193], with a thickness of 656 nm, exhibited a permeability to H_2 of 261 Barrer and ideal selectivities H_2/N_2, H_2/CO and H_2/CO_2 of ∞, ∞ and 7, respectively. Ultra-thin (~1 μm) palladium membranes, supported by a nickel micro-structured support grid were prepared by Dunbar et al. [194] and tested for their poisoning resistance to H_2 streams containing CO_2, CO and H_2O vapour in the temperature range 235–320 °C. At all temperatures, the rate-limiting hydrogen flux steps were found to be the surface reactions and not the atomic hydrogen sorption-diffusion though the bulk of the membranes. The deleterious effect of contaminant gases was found to be magnified by the fact that these adsorb on the palladium surface directly interfering with the rate limiting hydrogen flux step. Harmful diffusion of nickel from the micro-structured support grid into the palladium membrane was observed at temperatures above 360 °C.

Theoretical studies

On the theoretical and computational side, some very recent studies are worth mentioning. Liu et al. [195] used *ab initio* density functional theory (DFT) calculations to perform a

Please cite this article as: Bernardo G et al., Recent advances in membrane technologies for hydrogen purification, International Journal of Hydrogen Energy, https://doi.org/10.1016/j.ijhydene.2019.06.162

Table 1 – Properties of the Pd –based membranes with the highest separation performances.

Membrane Type	Preparation method	Operating Temperature (°C)	Δp (bar)	Thick (μm)	J_{H2} ($mol \cdot m^{-2} \cdot s^{-1}$)	H_2 permeance ($mol \cdot m^{-2} \cdot s^{-1} \cdot Pa^{-1}$)	$\alpha_{H2/X}$		Obs.	Year	Ref.
Ru/Pd/Al_2O_3/PSS 95% Pd – 5% Ru	ELP	180	1	15	1.8[a]	–	>4000	X = He	Stable over a period of 1200 h	2017	[174]
		450	1		6.8[a]		1150		–		
Au. $Pd_{91.7}Ag_{4.8}Au_{3.5}/ZrO_2$ ceramic porous tubes	ELP	400	1	2.71	0.32	2.52×10^{-3}[b]	–	–	–	2017	[175]
		450			0.42	3.21×10^{-3}[b]	–	–	–		
		500			0.48	3.69×10^{-3}[b]	–	–	–		
		550			0.54	4.27×10^{-3}[b]	–	–	–		
		600			0.63	4.71×10^{-3}[b]	~350	X = N_2	–		
Au. $Pd_{91.5}Ag_{4.7}Au_{3.8}/ZrO_2$ ceramic porous tubes		550		3.13	0.25	2.32×10^{-3}[b]	>4115		H_2S treatment: 9 ppm (85% recovery) $\alpha_{H2/N2}$ = 793 (after H_2S test)		
Au. $Pd_{90.5}Ag_{4.6}Au_{4.9}/ZrO_2$ ceramic porous tubes		550		2.31	0.45	3.91×10^{-3}[b]	>2557		H_2S treatment: 17 ppm (85% recovery) $\alpha_{H2/N2}$ = 121 (after H_2S test)		
OXI-CeO_2/Pd	ELP-PP	350–450	1–2	15.4	0.03–0.12	$4.74–6.35 \times 10^{-4}$[b]	10,000	X = N_2	–	2019	[179]
Pd/Al_2O_3/Pd	ELP	500	1	3.8[c]/2.5[d]	0.21	10.1×10^{-9}[b]	14,429	X = N_2	Pd double layer. H_2/N_2 selectivity increase with the increase of temperature.	2018	[180]
Pd/Al_2O_3	ELP	500	1	6 (Pd)	0.205	–	886	X = N_2	Without protective film	2017	[183]
TS-1-Pd/Al_2O_3		500	1	6 (Pd) + 2 (TS-1)	0.054		268		TS-1 is a zeolite protective film. Stable for 10 days of H_2 permeation at 500 °C and 5 days at 200 °C		
$Pd_{95}Ag_5/Al_2O_3$	ELP	400	1	1	0.46	4.6×10^{-6}	25,938	X = N_2		2018	[186]
YSZ-Al_2O_3/PdAg/ Hastelloy X	ELP	400–500	4	4	–	1.43×10^{-6}	3,500,000	X = N_2	$\alpha_{H2/N2}$ = 2,700,000 after 615 h. YSZ-Al_2O_3 is a porous protective layer	2018	[187]
PdAg/Hastelloy X		400–500	4	4	–	1.2×10^{-6}	93,300		$\alpha_{H2/N2}$ = 1,000 after 615 h. Without protective layer is much less stable.		
Pd–Ag/ZrO_2	PVD-ELP	400	1	1	–	800×10^{-8}	500	X = N_2	Ultra-thin supported membrane	2016	[189]
Pd–Ag/Hastelloy X	ELP	400	1	~4–5	–	100×10^{-8}	>200,000	X = N_2	–	2016	[190]
Pd–Ag	ELP	400	1	1.29	–	9×10^{-6}	3300	X = N_2	$\alpha_{H2/N2}$ = 1900 after 1000 h	2017	[191]
		400	1	0.46	–	15.3×10^{-6}	48		–		

[a] $m^3 m^{-2} h^{-1}$.
[b] $mol\ s^{-1} m^{-2} Pa^{-0.5}$.
[c] Outside Pd layer.
[d] Inside Pd layer.

Please cite this article as: Bernardo G et al., Recent advances in membrane technologies for hydrogen purification, International Journal of Hydrogen Energy, https://doi.org/10.1016/j.ijhydene.2019.06.162

comparative and systematic study of the temperature-dependency of the solubility, diffusivity, and permeability to hydrogen of body-centred cubic (BCC) PdCu and face-centred cubic (FCC) PdCu alloys and pure FCC Pd phases. The same authors, using DFT calculations, also studied the effects of Ag addition on phase stability, solubility, diffusivity and permeability to hydrogen of Pd_8Cu_8 phases with BCC and FCC structures [196]. DFT calculations were also used by Kumar et al. [197] to study all the steps involved in the permeation of H through a model PdCu membrane. Depending on the operation temperature and membrane thickness, it was found that the permeation can be limited by diffusion of H in the membrane bulk (low temperatures and thick membranes) or by the reassociation of atomic H to form H_2 on the permeate side of the membrane (high temperatures and thin membranes). On a different theoretical level, Zhao et al. [198] developed a thermodynamic model to predict the surface segregation of palladium-based binary alloys in vacuum and in a gas environment. The model was validated comparing theoretical predictions with experimental data from literature, showing a good semi-quantitative agreement. The model can therefore be used as a basic guideline to design novel Pd alloys for hydrogen separation membranes.

Section conclusions

In conclusion, palladium-based membranes besides offering excellent hydrogen selectivity, can be used in membrane reactors, providing the possibility to combine both the chemical reaction for hydrogen production and the purification step in a unique system. However, these membranes still display a relatively low hydrogen permeation flux; they cannot be used at low temperatures due to the "hydrogen embrittlement" phenomenon and they are very susceptible to chemical poisoning by contaminants such as CO and H_2S. Furthermore, due to the scarcity of palladium resources in the planet, it is a very expensive metal and the large scale industrial purification of H_2 using palladium membranes seems to be unfeasible. Therefore, in the future hydrogen economy, Pd membranes will most likely find their niche market in small scale and portable H_2 purification systems [188].

Electrochemical hydrogen pumping membranes (EHPM)

General overview

Electrochemical hydrogen pumping (EHP) with proton exchange membranes was discovered, during the development of Nafion®-type membranes for fuel cells, and first reported in the 1960s [199,200]. At that time, there was no economic interest in this discovery and it remained, for several decades, as a mere academic curiosity with no materialized applications. Meanwhile, the increasing interest in hydrogen-related technologies, associated with the progress in fuel cells [201–205], have made EHP both economically interesting and technically feasible. Contrary to fuel cells and electrolysis, the chemical reaction involved in EHP does not deliver neither energy, nor new products: simply hydrogen goes in and hydrogen goes out and is suitable for hydrogen purifications even when present at very low concentrations [206,207].

As shown in Fig. 3, the basic working principle of an EHP is that a multicomponent stream containing H_2 is directed into the anodic compartment of an electrochemical cell, where the hydrogen molecules are oxidized (equation (2)) in the catalyst layer of a porous electrode. Due to the applied potential difference, the resultant protons are then selectively "pumped" across a proton-conducting membrane, while the electrons go to the cathode through the external circuit. Finally, the protons and electrons recombine at the cathode producing molecular hydrogen (equation (3)).

$$\text{Anode: } H_2(g) \rightarrow 2H^+ + 2e^- \quad (2)$$

$$\text{Cathode: } 2H^+ + 2e^- \rightarrow H_2(g) \quad (3)$$

The potential difference between anode and cathode is given by equation (4), where ΔE_{Nernst} is given by the Nernst equation (5). More theoretical details can be found elsewhere [208].

$$\Delta E = \Delta E_{Nernst} + \eta_{\Omega} + \eta_{activation} \quad (4)$$

$$\Delta E_{Nernst} = \frac{RT}{2F} \ln \frac{p_{cathode}}{p_{anode}} \quad (5)$$

Devices operating at different temperature ranges have been used or are under development for EHP applications. Low temperature devices operate typically in the temperature range 50–80 °C. A major disadvantage of low temperature devices is their low electrode tolerance to contaminants, such as carbon monoxide, resulting in a reversible loss of performance. Another disadvantage is that the membranes in these devices need to be hydrated to guarantee proton conduction and there is a tendency of water flooding at the cathode side. These problems severely limit the utility of such devices in hydrogen separation and purification applications. These disadvantages can be, at least partially overcome through the use of higher temperature devices. Notably, operating at higher temperatures increases the platinum catalyst tolerance to carbon monoxide and other impurities [201]. Furthermore, in higher temperature devices flooding of the electrodes with water is minimized, as water exists only in the gas phase under normal operating conditions.

Multiple proton-conducting membranes have been proposed for EHP applications, including perfluorinated sulfonic acid (PFSA) polymers for low temperature devices (typically ~50–80 °C); phosphoric acid-doped polybenzimidazole (PBI) at intermediate temperatures (~160–180 °C); super-protonic solid acids at slightly higher temperatures (~250 °C) and proton-conducting oxide membranes at very high temperatures (>500 °C). This technology heavily borrows from the developments on materials and devices for PEM fuel cells. In fact, most of the current research in EHP, is focused on fundamental studies aiming at understanding the applicability of fuel cell membranes for EHP applications. The performance of various types of proton exchange membranes used in EHP are briefly reviewed below and summarized in Table 2. Due to the relatively low level of maturity of EHP

Please cite this article as: Bernardo G et al., Recent advances in membrane technologies for hydrogen purification, International Journal of Hydrogen Energy, https://doi.org/10.1016/j.ijhydene.2019.06.162

technology for H_2 purification, no economic assessments of the use of this technology are known in the literature.

Perfluorinated sulfonic acid (PFSA) membranes

The most well-known cation exchange perfluorinated membranes are Nafion®. Nafion microstructure combines hydrophobic domains (Teflon-like backbone), responsible for the material's morphological stability, with hydrophilic domains (sulfonate-HSO_3-end groups), where the transport of protons and water takes place [209]. Nafion membranes usually display high proton conductivities (in the order of 10^{-2} S cm^{-1} [210]). However, since this high proton conductivity heavily relies on the hydration of the membrane, the operation temperature is usually limited to ~80 °C to avoid a decrease of the moisture level [211].

Lee et al. [212] studied hydrogen purification from a $H_2/N_2/CO_2$ mixture, over a temperature range of 30–70 °C and over a feed pressure range of 1–3 atm, using a Nafion 115 membrane. Hydrogen purity was found to increase with the current density and with the temperature of the cell. The power efficiency reaches a maximum value at 300 mA cm^{-2} and increases with temperature and feed pressure. Gardner et al. [213] evaluated the feasibility of separating electrochemically, at room temperature, H_2 from a binary H_2:CO_2 gas mixture and from a ternary H_2:CO_2:CO gas mixture, using a EHP with a Nafion-115 membrane. Although the H_2 extraction efficiency from the binary gas mixture was quite high, with the ternary gas mixture was quite low. Periodic pulsing of the anode potential was shown to improve the efficiency of H_2 separation from the ternary H_2:CO_2:CO mixture. The efficiency of H_2 recovery from mixtures with CO_2 and H_2O, using a EHP with a Nafion-115 membrane, both single and multistage design, were studied by Abdulla et al. [214], at the temperatures of 50 and 70 °C. More recently, Hao et al. [215] reported a EHP, based on a Nafion-117 membrane, with an internal humidifier which consists of a vessel containing liquid water built in the cathode end plate, allowing the water to directly wet the Nafion-117 membrane. The conductivity was found to be higher than using a conventional vapour humidifier. Further studies of EHP based on PFSA membranes can be found in some additional references [216–219].

In the EHP studies using PFSA membranes, reported in this section, the morphology of the membranes has not received attention. However, the morphology of PFSA membranes has been the subject of a large number of studies performed mostly during the last two decades, using electron microscopy and advanced X-ray and neutron scattering techniques, and these have been recently reviewed, very proficiently, elsewhere [220]. The X-ray and neutron scattering spectra of PFSA membranes usually display a very characteristic broad ionomer peak corresponding to a structural correlation length for hydrophilic domains, and interpreted as the spacing between water domains on the nanometer range. The basic understanding is that a hydrated PFSA membrane exhibits nanoscale phase separation with various disordered complex morphologies forming a mesoscale connectivity with a hydrophilic ion-conducting phase and a hydrophobic, nonconductive phase controlling the mechanical integrity.

Polybenzimidazole (PBI) membranes

Phosphoric acid-doped PBI membranes provide efficient proton conductivity in the absence of water, at temperatures ~160–180 °C, while also guaranteeing good mechanical and thermo-chemical stability [221–223]. In these membranes, PBI provides the mechanical support of the membrane and the H_3PO_4 is responsible for the proton conductivity. Perry et al. [224] reported EHP at temperatures > 140 °C using a phosphoric acid-doped PBI membrane prepared by sol-gel. The device was used to purify H_2 from gas mixtures containing various amounts of CO and CO_2 and significant reductions in gas impurities were successfully achieved. The long-term durability of the membrane was demonstrated with a test that extended for nearly 4000 h. Thomassen et al. [225] demonstrated the H_2 purification, from N_2/H_2 mixtures and reformate feed gas mixtures containing various amounts of CO, CO_2 and CH_4, using an EHP with a PBI-based membrane and operating at temperatures > 100 °C. The process required relatively low energy consumption and demonstrated a good dynamic response. EHPs using phosphoric acid doped PBI membrane, were tested by Kim et al. [226] to concentrate CO_2 and produce pure H_2, from anode outlet gases (H_2/CO_2 mixture) of molten carbonate fuel cells (MCFC). The PBI-based hydrogen pump without humidification (160 °C) was shown to provide higher hydrogen separation performances (applied voltage of only 80 mV at 0.8 A/cm^2 for pure hydrogen feed) than a reference EHP with perfluorosulfonic-acid membranes at a relative humidity of 43% (80 °C). Study of the effect on performance of Pt loading on the anode and cathode showed that anodic hydrogen oxidation is predominant at determining the device's performance.

PBI is an essentially amorphous polymer, as measured by X-ray diffraction [222], and has a very high glass transition temperature (T_g) of about 425 °C and no melting point [227]. When doped with H_3PO_4, a decrease in T_g is observed due to the plasticizing effect of H_3PO_4. Infrared absorption can be used to follow PBI doping with H_3PO_4 due to the appearance of a very broad infrared absorption band in the range from about 2400 to 3000 cm^{-1}, corresponding to the protonation of the nitrogen of the imide by transferring one or more protons from H_3PO_4 to imidazole groups of PBI [222]. The morphology of phosphoric acid doped PBI membranes has been studied in-situ, using advanced synchrotron X-ray techniques, but these studies where performed during their operation in fuel cells [221] and not in EHPs.

Other polymeric membranes

Other polymeric membranes have been studied, for low-temperature hydrogen pumping applications, for being more cost-effective alternatives to perfluorinated sulfonic acid membranes. Sulfonated poly (ether-ether-ketone) (SPEEK) membranes and sulfonated poly (phthalazinone-ether-sulfone-ketone) (SPPESK) membranes are two notable examples. The X-ray and neutron scattering spectra of these membranes also display the characteristic ionomer peak corresponding to a correlation length between hydrophilic domains in the hydrated state [228]. However, according to previous reports [229], compared to PFSA membranes the ionomer peak is

Please cite this article as: Bernardo G et al., Recent advances in membrane technologies for hydrogen purification, International Journal of Hydrogen Energy, https://doi.org/10.1016/j.ijhydene.2019.06.162

shifted towards higher scattering angles which indicates a smaller characteristic separation length and a larger interface between the hydrophilic and hydrophobic domains.

Wu et al. [230] demonstrated a EHP for H_2 purification from a H_2/CO_2 mixture, using a SPEEK/cross-linked poly (styrene sulfonic acid) (CrPSSA) semi-interpenetrating polymer network membrane. The SPEEK/CrPSSA membrane showed a higher proton conductivity and humidity sensitivity than the pristine SPEEK membrane. The energy efficiency of the SPEEK/CrPSSA-based hydrogen pump was found to be ~30%, which compares with the value of ~40% reported in the literature for Nafion-based hydrogen pumps. A EHP using a sulfonated poly (phthalazinone-ether-sulfone-ketone) (SPPESK) was successfully tested by Huang et al. [231] for the purification of H_2 from H_2/CO_2 mixtures, achieving a H_2 purity greater than 99.99%. In addition, compared to Nafion-membranes, the lower permeability to CO_2 of the SPPESK membrane led to less poisoning of the Pt cathode catalyst. Very recently, Rico-Zavala et al. [232] tested the incorporation in a EHP of a SPEEK-based composite membrane modified with Halloysite nanotubes (HNT) and HNT impregnated with phosphotungstic acid fillers ($H_3PW_{12}O_{40}\cdot nH_2O$, PWA), PWA/HNT30. For the case of PWA/HNT30, SEM-EDS and X-ray diffraction (XRD) analysis show that the PWA fillers distribute and recrystallize uniformly over the nanotubes. This helps improving the dispersion of the nanotubes in the polymer matrix as well as the mechanical and structural stability of the membrane. Compared to the unmodified membrane, the composite membrane with PWA/HNT30 displayed reduced swelling and increased proton conductivity and consequently this composite-based EHP presented a lower energy consumption and a lower crossover at high current densities.

Superprotonic solid acids

Caesium dihydrogen phosphate, CsH_2PO_4, is a superprotonic solid acid that has attracted significant interest as it can operate in fuel cells and EHPs at temperatures of ~250 °C. CsH_2PO_4 undergoes a polymorphic structural transition upon heating at ~230 °C [233–235], known as superprotonic phase transition, in which the proton conductivity increases by several orders of magnitude to a value of ~2.2×10^{-2} S cm^{-1} at 240 °C [236]. Papandrew et al. [237,238] investigated CsH_2PO_4 as a proton exchange membrane for electrochemical hydrogen separation at temperatures from 230 °C to 250 °C. Vapour-grown carbon-supported Pt and Pd catalysts [237] were evaluated as hydrogen oxidation catalysts in hydrogen pump electrodes and their performances were found to be virtually identical. Hydrogen oxidation and evolution reactions were reversible on 100% H_2, and a cell current of 300 mA cm^{-2} was produced at a 25 mV overpotential after correction for the membrane ohmic resistance. Unsupported Ni catalyst was tested in an EHP using CsH_2PO_4 as a proton exchange membrane and compared to a similar Pt-based EHP control [238]. Ni-based electrodes display a proton reduction current of 207 mA cm^{-2} at a −0.2 V cell potential, in humidified hydrogen at 250 °C. Pt-based electrodes evolved H_2 at 558 mA cm^{-2} under identical conditions. Hydrogen oxidation activity was virtually absent on Ni.

Proton-conducting oxide membranes

Proton-conducting oxide [239] membranes work at high temperatures, typically ~800–900 °C, and have also been the subject of research for EHP. In 1986, Iwahara et al. [240] studied the extraction of H_2 from the gas mixture of the shift reaction using a proton-conducting oxide membrane with chemical composition $SrCe_{0.95}Yb_{0.05}O_{3-\alpha}$ (where α denotes the amount of oxygen vacancy) at 800–900 °C. Although at relatively low current densities, the hydrogen extraction rate was close to the theoretical value calculated from Faraday's law, at higher current densities the hydrogen extraction rate reached a limiting value. Later, the same authors were able to extract H_2 from hydrocarbon-hydrogen mixtures using a $BaCe_{0.90}Nd_{0.10}O_{3-\alpha}$ membrane as electrolyte, working at 650 °C [241]. The H_2 evolution rate obeyed Faraday's law when the current density was lower than some critical value which depended on the electrode condition. Matsumoto et al. [242], in the year 2000, studied electrochemical H_2 pumping from wet hydrogen gas, at the very

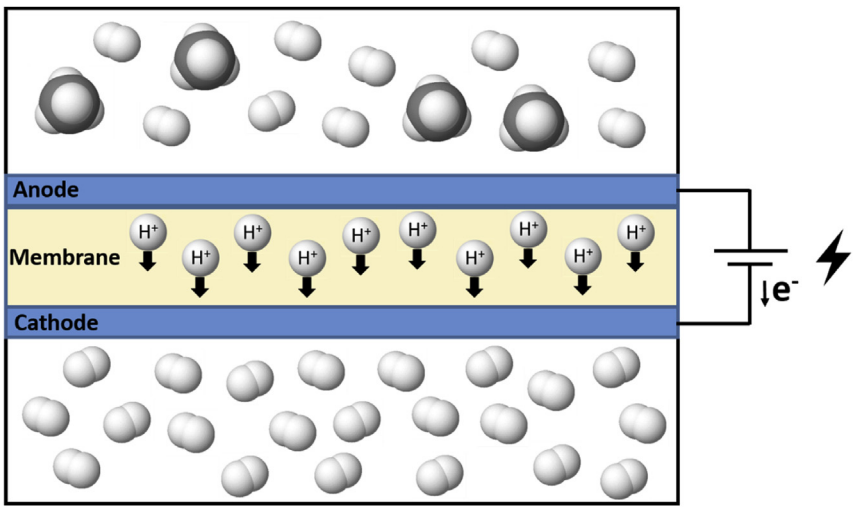

Fig. 3 – Schematic diagram of the working principle of an EHP.

Please cite this article as: Bernardo G et al., Recent advances in membrane technologies for hydrogen purification, International Journal of Hydrogen Energy, https://doi.org/10.1016/j.ijhydene.2019.06.162

Table 2 – Performance of several proton exchange membranes in hydrogen pumping applications.

Membrane Electrode Assembly (MEA)		Operating conditions			Performance in EHP	Ref. (year)
Membrane (thickness)	Electrodes (active area)	Temp. (°C)	Feed	Applied Voltage or Applied Current density		
Catalytic electrodes of platinum-supported active carbon on porous carbon matrix		30	12.5% H_2/87.5% N_2	200 mA cm^{-2}	Production: approx. 1.6 $ml_{H2} \cdot min^{-1}$ per cm^2 of cell area	[200] (1965)
Perfluorinated sulfonic acid (PFSA) membranes						
Catalyst-loaded (0.2 $mg_{Pt} \cdot cm^{-2}$) Nafion© (0.254 mm)	Platinum (46.6 cm^2)	25	30% H_2/70% N_2 (Total pressure of 100 kPa)	300 mA cm^{-2}	H_2 was purified and pressurized from 29.6 kPa to 792 kPa; Voltage efficiency: 87%	[216] (1981)
Catalyst-loaded (0.4 $mg_{Pt} \cdot cm^{-2}$) Nafion© 115 (0.127 mm)	Graphite (1.9 cm^2)	50	CO_2/H_2/H_2O mixture (6.3 ml min^{-1} cm^{-2}, (C/H) = 0.5)	(1) Single stage fixed $V_{applied}$ = 0.45 V; (2) 20 stage, fixed $V_{applied}$ = 0.3 V; (3) 20 stage, variable $V_{applied}$ = 0.65 -> 0.02 V	Hydrogen purity: >99.99%; Hydrogen recovery and Energy efficiency: (1) 62.3%, 44.2% (2) 96.8%, 73.6% (3) 98.25%, 92.6%	[214] (2011)
Nafion© 117 membrane	Carbon-supported platinum (25 cm^2)	35	100% H_2 at atmospheric pressure	200 mA cm^{-2}	With required cell voltage of 140 mV, hydrogen was pressurized from 101 kPa to 4800 kPa; Energy consumption: *ca.* 0.3 kWh Nm^{-3}	[218] (2011)
Polybenzimidazole (PBI) membranes						
Phosphoric acid-doped PBI (approx. 0.250 mm)	Etek (1.0 $mg_{Pt} \cdot cm^{-2}$, 10 cm^2)	160	35.8% H_2/11.9% CO_2/1906 ppm CO and N_2 balance	400 mA cm^{-2}	Impurities in Cathode outlet: 0.37 ± 0.09% CO_2/ 11 ± 1 ppm CO; Long-term durability demonstrated in a test that extended 4000 h	[224] (2008)
Phosphoric acid-doped PBI (0.025 mm)	Pt/C (1.1 $mg_{Pt} \cdot cm^{-2}$, 25 cm^2)	160	Non-humidified (1) 100% H_2, (2) H_2/CO_2 mixture (2:8); 480 ml min^{-1}	800 mA cm^{-2}	Required cell voltage of (1) 0.080 V, (2) 0.205 V	[226] (2013)
Other polymeric membranes						
(1) SPEEK, (2) SPEEK(HNT), (3) SPEEK(PWA/HNT30)	Pt/C (0.5 $mg_{Pt} \cdot cm^{-2}$, 25 cm^2)	25	Humidified H_2; 260 ml min^{-1}	400 mA cm^{-2}	Proton conductivity (100% relative humidity): (1) 0.01158 S cm^{-1}, (2) 0.01967 S cm^{-1}, (3) 0.02037 S cm^{-1}; At high current densities (>400 mA cm^{-2}), composite membranes (2) and (3) demonstrated lower hydrogen crossover and lower energy consumption than (1)	[232] (2018)
SPEEK/CrPSSA sIPN (0.100 mm)	Pt/C (0.5 $mg_{Pt} \cdot cm^{-2}$, 1.9 cm^2)	80	Humidified 80% H_2/20% CO_2 gas mixture; 16 ml min^{-1}	–	Proton conductivity: 0.08–0.1 S cm^{-1}; Energy efficiency of ~30%	[230] (2014)
SPPESK (0.070 mm)	Pt/C (0.5 $mg_{Pt} \cdot cm^{-2}$, 1.9 cm^2)	40	Dry 25% H_2/75% CO_2 gas mixture; 50 ml min^{-1}	56.7 mA cm^{-2}	Proton conductivity: 0.0338 S cm^{-1}; Outlet stream: >99.99% H_2; Energy efficiency: 35% at 60% hydrogen recovered; Higher CO_2 poisoning resistance than Nafion	[231] (2016)

Please cite this article as: Bernardo G et al., Recent advances in membrane technologies for hydrogen purification, International Journal of Hydrogen Energy, https://doi.org/10.1016/j.ijhydene.2019.06.162

Super protonic solid acids						
CsH_2PO_4 (0.070 mm)	(1) Pt/C (0.5 $mg_{Pt} \cdot cm^{-2}$, 1.35 cm^2); (2) Ni/C (3.5 $mg_{Ni} \cdot cm^{-2}$, 1.35 cm^2);	250	100% H_2; 30 sccm	0.2 V	Proton conductivity: 0.025 S cm^{-1}; Resulting current densities of (1) 588 mA cm^{-2} and (2) 207 mA cm^{-2}	[238] (2014)
Proton-conducting oxide membranes						
$SrCe_{0.95}Yb_{0.05}O_{3-\alpha}$ (0.500 mm)	Porous Platinum	900	CO/H_2O gas mixture (101 kPa); $P_{H2O} \approx 7.1$ kPa	100 mA cm^{-2}	Production: 0.5 $ml_{H2} \cdot min^{-1} \cdot cm^{-2}$	[240] (1986)
$La_{0.9}Ba_{0.1}YbO_{3-\alpha}$, LBYb-91 (0.500 mm)	Porous Palladium	800	Humidified H_2; $P_{H2O} = 1.9$ kPa	40 mA cm^{-2}	Conductivity: 0.0042 S cm^{-1}; High chemical stability towards CO_2 and H_2O	[245] (2013)
$Ba(Zr_{0.30}Ce_{0.54}Y_{0.15}Cu_{0.01})O_{3-\delta}$ (0.085 mm)	Sr-doped $LaVO_3$ and Cu and Y-doped $Ba(Ce,Zr)O_3$] (both 0.080 mm)	(1)600 (2)700	Humidified 50% H_2 gas mixture balanced with He; 10 sccm	1000 mA cm^{-2}	Faraday efficiency of 84%; Required cell voltage of (1) 1.07 V, (2) 0.51 V	[246] (2017)

high temperature of 900 °C, using a membrane of $SrCe_{0.95}Yb_{0.05}O_{3-\alpha}$. A decrease in hydrogen evolution rate was observed at relatively high current densities (>90 mA cm^{-2}). An increase in the amount of H_2O vapour in the anode H_2 gas caused a decrease in the critical current density for the reduction of the cell efficiency. The performance of EHPs, operating at 800 °C, using $SrZr_{0.9}Y_{0.1}O_{3-\alpha}$ (10Y-SZO) and $SrZr_{0.5}Ce_{0.4}Y_{0.1}O_{3-\alpha}$ (10Y-SZCO) as proton-conducting electrolytes, and electroless-plated and screen-printed pasted platinum electrodes, were tested by Sakai et al. [243]. SEM analysis showed that the electroless-plated electrodes have a dense structure with little porosity contrary to the pasted electrodes that are formed by platinum grains of several micrometers in grain size. In the case of the EHPs with plated platinum electrodes, using both electrolytes, the H_2 evolution rates agreed well with Faraday's law up to a current density of 270 mA cm^{-2}. On the other hand, in the case of the EHPs with pasted electrodes, using both electrolytes, the H_2 evolution rates began to deviate from Faraday's law at much lower current densities. Therefore, the authors concluded that the performance of the EHPs was clearly improved with the use of plated platinum electrodes in place of pasted ones. In another work, Sakai et al. [244] studied EHPs operating at 800 °C using a $SrZr_{0.9}Y_{0.1}O_{3-\alpha}$ (SZY-91) membrane combined with palladium electrodes prepared either by sputtering or by screen printing followed by baking. The hydrogen evolution rate of the sputtered palladium electrode cell followed Faraday's law up to 180 mA cm^{-2}, and electrode overpotentials were significantly lower than those of a similar platinum electrode cell, suggesting that the palladium electrode is effective to improve the performance of the hydrogen-pumping cell using $SrZrO_3$-based electrolyte. It was also observed that the screen-printed palladium electrodes become denser when baked at higher temperature (1400 °C) and that higher performance was obtained by the denser electrode than by the more porous electrode baked at 950 °C. Later, the same authors tested EHPs [245] at 600 °C and 800 °C, using as proton conductor membrane a Ba doped $LaYbO_3$ oxide ($La_{0.9}Ba_{0.1}YbO_{3-\alpha}$, LBYb-91), which has the highest proton conductivity among LaYbO3 series oxides. For anode and cathode, porous palladium electrodes were prepared by screen-printing and then fired at 1400 °C. LBYb-91 demonstrated a high chemical stability towards CO_2 and H_2O, as evaluated by using powder XRD and thermal gravimetric analysis. The H_2 evolution rates of the LBYb-91 cell obeyed Faraday's law at both temperatures (600 °C and 800 °C). The LBYb-91 cell showed about 0.7 V at 40 mA cm^{-2}, which is comparable with the cell using SZY-91 with porous palladium electrode. It was concluded that LBYb-91 is a potential candidate electrolyte material for the EHP cell for the H_2 separation from the reformed gas. More recently, in 2017, Choi et al. [246] studied a hydrogen pump, operating at 700 °C, using a 85 μm-thick dense protonic ceramic electrolyte with chemical composition $Ba(Zr_{0.30}Ce_{0.54}Y_{0.15}Cu_{0.01})O_{3-\delta}$ and two porous ceramic composite electrodes, 80 μm-thick each, comprising an electron-conducting ceramic (Sr-doped $LaVO_3$), a protonic ceramic [Cu and Y-doped $Ba(Ce,Zr)O_3$], and small amounts of CeO_2 and Pd as catalysts. This hydrogen pump performed well and exhibited an overpotential of only ~1.1.V at a large current density of 2 A cm^{-2}. This good

performance was attributed mainly to the ceramic composite electrode fabricated by an infiltration method.

Section conclusions

EHPM can offer high selectivity, high hydrogen permeation and relatively low energy consumption. Although the technology remains expensive due to the use of precious metals (Pt) as electrocatalyst and use of expensive proton-conductor membranes, it will certainly profit from progresses made in the related PEM fuel cell and water electrolysis technologies which use similar cell components. Therefore, further efficiency improvements and cost reductions are expectable in the near future making this technology attractive particularly for medium sized production sites and point-of-use applications. Furthermore, in the near future, the H_2 produced in large quantities will need to be transported for long distances and the use of the existing natural gas pipelines is considered the best transport option [247–251]. In this context, EHPs will be expected to play an important role in the extraction of H_2 from gas mixtures in natural gas pipelines because EHPs do not require a driving pressure differential. In EHPs, electricity is the driving force that can produce pure H_2 at a higher pressure than the incoming feedstock gas.

General conclusions

Membrane separation technology is set to play a crucial role in the future of industrial H_2 purification. Although a wide variety of membrane types can be used for hydrogen separation and purification, in this review we focused on four types that we consider more promising for H_2 purification, namely: CMSM; ionic-liquid based membranes; palladium-based membranes and EHPM.

CMSM rely on the molecular sieving mechanism and with permeability-selectivity values frequently exceeding the well-known Robeson upper boundary, they are very promising candidates for hydrogen separation over a wide range of temperatures. Different strategies have been tested for improving the H_2 separation performance of CMSMs and these include: changing carbonization conditions; blending of polymer precursors; addition of inorganic fillers and metal nanoparticles to the polymer precursors; changing of membrane-support interfacial effects and post-treatment effects. However, CMSMs perform poorly on the separation of H_2/CO_2 mixtures and despite being resistant to CO and sulphur poisoning, their high brittleness and vulnerability to humidity has so far seriously limited their commercialization.

Ionic-liquid based membranes operate through a sorption-diffusion mechanism and seem particularly well suited for addressing one of the major weaknesses of CMSMs, namely the separation of H_2 from CO_2. There are several different types of ionic-liquid based membranes, namely: supported ionic liquid membranes (SILMs); polymer-IL composite membranes; polymer-IL gel membranes and polymerized ionic liquid membranes (PILM). Some of the best ionic-liquid based membranes reported so far displayed permeabilities to CO_2 > 1000 Barrer and CO_2/H_2 ideal selectivities >10. Although these values are still well below the industrial requirements, as the technology is still very new the potential for their optimization and improvement is still very high.

Palladium-based membranes are, compared to the others, at a more advanced stage of development and have already some industrial implementation. They operate through a sorption-diffusion mechanism and despite their extremely high selectivity to H_2, they are very prone to chemical contamination by CO and sulphur compounds. Furthermore, palladium is a scarce and expensive metal which severely limits their widespread use in large scale industrial applications. Recent studies have mostly been focused in: alloying palladium with other metals to reduce the price and increase the chemical resistance of the membranes; depositing porous protective layers (zeolite, ceramic) on the surface of the membranes to increase their chemical resistance and developing ultra-thin cost-effective membranes with very high hydrogen permeation flux.

EHPM are proton-conducting membranes that depending on the operating temperature conditions can be made of several different materials including: PFSA; PBI; other polymeric materials such as sulfonated poly (ether ether ketone) (SPEEK); superprotonic solid acids and oxide membranes based mostly on Ba, Sr and La. Although these membranes can offer high selectivity, high hydrogen flux and relatively low energy consumption, they are still expensive due to the use of precious metals, such as platinum, as electro-catalyst.

Acknowledgements

This work was financially supported by project UID/EQU/00511/2019 - Laboratory for Process Engineering, Environment, Biotechnology and Energy – LEPABE funded by national funds through FCT/MCTES (PIDDAC).

This work was also financially supported by: Project PTDC/EQU-EQU/30760/2017 - POCI-01-0145-FEDER-030760 - funded by FEDER funds through COMPETE2020 - Programa Operacional Competitividade e Internacionalização (POCI) and by national funds (PIDDAC) through FCT/MCTES.

Appendix A. Supplementary data

Supplementary data to this article can be found online at https://doi.org/10.1016/j.ijhydene.2019.06.162.

REFERENCES

[1] Al-Ghussain L. Global warming: review on driving forces and mitigation. Environ Prog Sustain Energy 2019;38(1):13–21.
[2] Cook J, et al. Consensus on consensus: a synthesis of consensus estimates on human-caused global warming. Environ Res Lett 2016;11(4):048002.
[3] Davy R, et al. Diurnal asymmetry to the observed global warming. Int J Climatol 2017;37(1):79–93.
[4] Capellan-Perez I, et al. Fossil fuel depletion and socio-economic scenarios: an integrated approach. Energy 2014;77:641–66.

[5] Höök M, Tang X. Depletion of fossil fuels and anthropogenic climate change—a review. Energy Policy 2013;52:797–809.
[6] Whiting K, Carmona LG, Sousa T. A review of the use of exergy to evaluate the sustainability of fossil fuels and non-fuel mineral depletion. Renew Sustain Energy Rev 2017;76:202–11.
[7] Wilberforce T, et al. Advances in stationary and portable fuel cell applications. Int J Hydrogen Energy 2016;41(37):16509–22.
[8] Wilberforce T, et al. Developments of electric cars and fuel cell hydrogen electric cars. Int J Hydrogen Energy 2017;42(40):25695–734.
[9] Chen HC, et al. A review of durability test protocols of the proton exchange membrane fuel cells for vehicle. Appl Energy 2018;224:289–99.
[10] Hanley ES, Deane JP, Gallachóir BPÓ. The role of hydrogen in low carbon energy futures–A review of existing perspectives. Renew Sustain Energy Rev 2018;82:3027–45.
[11] Staffell I, et al. The role of hydrogen and fuel cells in the global energy system. Energy Environ Sci 2019;12(2):463–91.
[12] Hosseini SE, Wahid MA. Hydrogen production from renewable and sustainable energy resources: promising green energy carrier for clean development. Renew Sustain Energy Rev 2016;57:850–66.
[13] Nikolaidis P, Poullikkas A. A comparative overview of hydrogen production processes. Renew Sustain Energy Rev 2017;67:597–611.
[14] Acar C, Dincer I. Review and evaluation of hydrogen production options for better environment. J Clean Prod 2019;218:835–49.
[15] da Silva Veras T, et al. Hydrogen: trends, production and characterization of the main process worldwide. Int J Hydrogen Energy 2017;42(4):2018–33.
[16] El-Shafie M, Kambara S, Hayakawa Y. Hydrogen production technologies overview. J Power Energy Eng 2019;7:107–54.
[17] Aziz M, Oda T, Kashiwagi T. Carbon-free hydrogen production from low rank coal. In: Nur A, Wijayanta AT, Budiman AW, editors. 3rd international conference on industrial, mechanical, electrical, and chemical engineering; 2018.
[18] Salkuyeh YK, Saville BA, MacLean HL. Techno-economic analysis and life cycle assessment of hydrogen production from natural gas using current and emerging technologies. Int J Hydrogen Energy 2017;42(30):18894–909.
[19] Nowotny J, et al. Towards sustainable energy. Generation of hydrogen fuel using nuclear energy. Int J Hydrogen Energy 2016;41(30):12812–25.
[20] Zhang P, et al. Streamlined hydrogen production from biomass. Nat Cataly 2018;1(5):332–8.
[21] Salkuyeh YK, Saville BA, MacLean HL. Techno-economic analysis and life cycle assessment of hydrogen production from different biomass gasification processes. Int J Hydrogen Energy 2018;43(20):9514–28.
[22] Correa CR, Kruse A. Supercritical water gasification of biomass for hydrogen production Review. J Supercrit Fluids 2018;133:573–90.
[23] Vilanova A, et al. Optimized photoelectrochemical tandem cell for solar water splitting. Energy Stor Mat 2018;13:175–88.
[24] Marchenko OV, Solomin SV. The future energy: hydrogen versus electricity. Int J Hydrogen Energy 2015;40(10):3801–5.
[25] Brandon NP, Kurban Z. Clean energy and the hydrogen economy. Phil Trans R Soc Mathemat Phys Eng Sci 2017;375(2098).
[26] Moliner R, Lázaro MJ, Suelves I. Analysis of the strategies for bridging the gap towards the hydrogen economy. Int J Hydrogen Energy 2016;41(43):19500–8.
[27] Moreno-Benito M, Agnolucci P, Papageorgiou LG. Towards a sustainable hydrogen economy: optimisation-based framework for hydrogen infrastructure development. Comput Chem Eng 2017;102:110–27.
[28] Ball M, Weeda M. The hydrogen economy – vision or reality? Int J Hydrogen Energy 2015;40(25):7903–19.
[29] Dincer I, Acar C. Innovation in hydrogen production. Int J Hydrogen Energy 2017;42(22):14843–64.
[30] Chen J, et al. Methane steam reforming thermally coupled with catalytic combustion in catalytic microreactors for hydrogen production. Int J Hydrogen Energy 2017;42(1):664–80.
[31] Cui X, Kær SK. Thermodynamic analysis of steam reforming and oxidative steam reforming of propane and butane for hydrogen production. Int J Hydrogen Energy 2018;43(29):13009–21.
[32] Nguyen DD, et al. Optimal design of a sleeve-type steam methane reforming reactor for hydrogen production from natural gas. Int J Hydrogen Energy 2019;44(3):1973–87.
[33] Sengodan S, et al. Advances in reforming and partial oxidation of hydrocarbons for hydrogen production and fuel cell applications. Renew Sustain Energy Rev 2018;82:761–80.
[34] Chen JJ, et al. Production of hydrogen by methane steam reforming coupled with catalytic combustion in integrated microchannel reactors. Energies 2018;11(8):2045.
[35] Abbas SZ, Dupont V, Mahmud T. Modelling of H_2 production via sorption enhanced steam methane reforming at reduced pressures for small scale applications. Int J Hydrogen Energy 2019;44(3):1505–13.
[36] Ngo SI, et al. Computational fluid dynamics and experimental validation of a compact steam methane reformer for hydrogen production from natural gas. Appl Energy 2019;236:340–53.
[37] Iulianelli A, et al. Advances on methane steam reforming to produce hydrogen through membrane reactors technology: a review. Catal Rev Sci Eng 2016;58(1):1–35.
[38] Soria MA, et al. COx free hydrogen production through water-gas shift reaction in different hybrid multifunctional reactors. Chem Eng J 2019;356:727–36.
[39] LeValley TL, Richard AR, Fan M. The progress in water gas shift and steam reforming hydrogen production technologies – a review. Int J Hydrogen Energy 2014;39(30):16983–7000.
[40] Pal DB, et al. Performance of water gas shift reaction catalysts: a review. Renew Sustain Energy Rev 2018;93:549–65.
[41] Seçer A, et al. Comparison of co–gasification efficiencies of coal, lignocellulosic biomass and biomass hydrolysate for high yield hydrogen production. Int J Hydrogen Energy 2018;43(46):21269–78.
[42] Hasanoğlu A, Demirci I, Seçer A. Hydrogen production by gasification of Kenaf under subcritical liquid–vapor phase conditions. Int J Hydrogen Energy 2019.
[43] Al-Rahbi AS, Williams PT. Hydrogen-rich syngas production and tar removal from biomass gasification using sacrificial tyre pyrolysis char. Appl Energy 2017;190:501–9.
[44] Sikarwar VS, et al. An overview of advances in biomass gasification. Energy Environ Sci 2016;9(10):2939–77.
[45] Sołowski G, et al. Production of hydrogen from biomass and its separation using membrane technology. Renew Sustain Energy Rev 2018;82:3152–67.
[46] Irfan M, et al. Production of hydrogen enriched syngas from municipal solid waste gasification with waste marble powder as a catalyst. Int J Hydrogen Energy 2019;44(16):8051–61.
[47] Couto N, et al. Hydrogen-rich gas from gasification of Portuguese municipal solid wastes. Int J Hydrogen Energy 2016;41(25):10619–30.

Please cite this article as: Bernardo G et al., Recent advances in membrane technologies for hydrogen purification, International Journal of Hydrogen Energy, https://doi.org/10.1016/j.ijhydene.2019.06.162

[48] Wang MY, et al. The intensification technologies to water electrolysis for hydrogen production - a review. Renew Sustain Energy Rev 2014;29:573–88.
[49] Chi J, Yu H. Water electrolysis based on renewable energy for hydrogen production. Chin J Catal 2018;39(3):390–4.
[50] dos Santos KG, et al. Hydrogen production in the electrolysis of water in Brazil, a review. Renew Sustain Energy Rev 2017;68:563–71.
[51] Shiva Kumar S, Himabindu V. Hydrogen production by PEM water electrolysis – a review. Mat Sci Energy Technol 2019.
[52] Carmo M, et al. A comprehensive review on PEM water electrolysis. Int J Hydrogen Energy 2013;38(12):4901–34.
[53] Muradov N. Low to near-zero CO_2 production of hydrogen from fossil fuels: status and perspectives. Int J Hydrogen Energy 2017;42(20):14058–88.
[54] Sinigaglia T, et al. Production, storage, fuel stations of hydrogen and its utilization in automotive applications-a review. Int J Hydrogen Energy 2017;42(39):24597–611.
[55] Standardization IOf. ISO 14687-2 - Hydrogen fuel — product specification — Part 2: proton exchange membrane (PEM) fuel cell applications for road vehicles. Switzerland: ISO copyright of International Organization for Standardization International Organization for Standardizationfice; 2012.
[56] Fraile D, et al. Overview of the market segmentation for hydrogen across potential customer groups, based on key application areas. 2015.
[57] Relvas F, et al. Single-stage pressure swing adsorption for producing fuel cell grade hydrogen. Ind Eng Chem Res 2018;57(14):5106–18.
[58] Ye F, et al. Artificial neural network based optimization for hydrogen purification performance of pressure swing adsorption. Int J Hydrogen Energy 2019;44(11):5334–44.
[59] Zhu X, et al. Elevated temperature pressure swing adsorption process for reactive separation of CO/CO_2 in H_2-rich gas. Int J Hydrogen Energy 2018;43(29):13305–17.
[60] Fakhroleslam M, Bozorgmehry Boozarjomehry R, Fatemi S. Design of a dynamical hybrid observer for pressure swing adsorption processes. Int J Hydrogen Energy 2017;42(33):21027–39.
[61] Shukla A, Sahoo S, Moharir AS. Non-isothermal Multi-cell Model for pressure swing adsorption process. Int J Hydrogen Energy 2017;42(8):5150–67.
[62] Wang B, et al. Evaluation of mass transfer correlations applying to cryogenic distillation process with non-equilibrium model. Cryogenics 2019;97:22–30.
[63] Yousef AM, et al. New approach for biogas purification using cryogenic separation and distillation process for CO_2 capture. Energy 2018;156:328–51.
[64] Bhattacharyya R, Bhanja K, Mohan S. Simulation studies of the characteristics of a cryogenic distillation column for hydrogen isotope separation. Int J Hydrogen Energy 2016;41(9):5003–18.
[65] Tarun CB, et al. Techno-economic study of CO_2 capture from natural gas based hydrogen plants. Int J Greenhouse Gas Contr 2007;1(1):55–61.
[66] Ji G, Zhao M. Membrane separation technology in carbon capture. In: Yun Y, editor. Recent advances in carbon capture and storage; 2017. IntechOpen: Croatia.
[67] Koresh J, Soffer A. Study of molecular sieve carbons. Part 1.—pore structure, gradual pore opening and mechanism of molecular sieving. J Chem Soc Faraday Trans 1 Phys Chem Condens Phases 1980;76(0):2457–71.
[68] Adams JS, et al. New insights into structural evolution in carbon molecular sieve membranes during pyrolysis. Carbon 2019;141:238–46.
[69] Kiyono M, Williams PJ, Koros WJ. Effect of pyrolysis atmosphere on separation performance of carbon molecular sieve membranes. J Membr Sci 2010;359(1):2–10.
[70] Xu LR, Rungta M, Koros WJ. Matrimid (R) derived carbon molecular sieve hollow fiber membranes for ethylene/ethane separation. J Membr Sci 2011;380(1–2):138–47.
[71] Parsley D, et al. Field evaluation of carbon molecular sieve membranes for the separation and purification of hydrogen from coal- and biomass-derived syngas. J Membr Sci 2014;450:81–92.
[72] He X. Techno-economic feasibility analysis on carbon membranes for hydrogen purification. Separ Purif Technol 2017;186:117–24.
[73] Llosa Tanco MA, Pacheco Tanaka DA. Recent advances on carbon molecular sieve membranes (CMSMs) and reactors. Processes 2016;4(3):29.
[74] Hamm JBS, et al. Recent advances in the development of supported carbon membranes for gas separation. Int J Hydrogen Energy 2017;42(39):24830–45.
[75] Saufi SM, Ismail AF. Fabrication of carbon membranes for gas separation - a review. Carbon 2004;42(2):241–59.
[76] Suda H, Haraya K. Gas permeation through micropores of carbon molecular sieve membranes derived from kapton polyimide. J Phys Chem B 1997;101(20):3988–94.
[77] Liu S, et al. Gas permeation properties of carbon molecular sieve membranes derived from novel poly(phthalazinone ether sulfone ketone). Ind Eng Chem Res 2008;47(3):876–80.
[78] Campo MC, Magalhães FD, Mendes A. Carbon molecular sieve membranes from cellophane paper. J Membr Sci 2010;350(1):180–8.
[79] Rodrigues SC, Whitley R, Mendes A. Preparation and characterization of carbon molecular sieve membranes based on resorcinol–formaldehyde resin. J Membr Sci 2014;459:207–16.
[80] Llosa Tanco MA, et al. Composite-alumina-carbon molecular sieve membranes prepared from novolac resin and boehmite. Part I: preparation, characterization and gas permeation studies. Int J Hydrogen Energy 2015;40(16):5653–63.
[81] Llosa Tanco MA, Pacheco Tanaka DA, Mendes A. Composite-alumina-carbon molecular sieve membranes prepared from novolac resin and boehmite. Part II: effect of the carbonization temperature on the gas permeation properties. Int J Hydrogen Energy 2015;40(8):3485–96.
[82] Favvas EP, et al. Helium and hydrogen selective carbon hollow fiber membranes: the effect of pyrolysis isothermal time. Separ Purif Technol 2015;142:176–81.
[83] Sá S, Sousa JM, Mendes A. Steam reforming of methanol over a $CuO/ZnO/Al_2O_3$ catalyst part II: a carbon membrane reactor. Chem Eng Sci 2011;66(22):5523–30.
[84] Rodrigues SC, et al. Preparation of carbon molecular sieve membranes from an optimized ionic liquid-regenerated cellulose precursor. J Membr Sci 2019;572:390–400.
[85] Rodrigues SC, et al. Carbon membranes with extremely high separation factors and stability. Energy Technol 2019;0(0).
[86] Zhou W, et al. Carbon molecular sieve membranes derived from phenolic resin with a pendant sulfonic acid group. Ind Eng Chem Res 2001;40(22):4801–7.
[87] Zhang X, et al. Carbon molecular sieve membranes derived from phenol formaldehyde novolac resin blended with poly(ethylene glycol). J Membr Sci 2007;289(1):86–91.
[88] Hosseini SS, Chung TS. Carbon membranes from blends of PBI and polyimides for N_2/CH_4 and CO_2/CH_4 separation and hydrogen purification. J Membr Sci 2009;328(1):174–85.
[89] Itta AK, Tseng H-H, Wey M-Y. Fabrication and characterization of PPO/PVP blend carbon molecular sieve membranes for H_2/N_2 and H_2/CH_4 separation. J Membr Sci 2011;372(1):387–95.

Please cite this article as: Bernardo G et al., Recent advances in membrane technologies for hydrogen purification, International Journal of Hydrogen Energy, https://doi.org/10.1016/j.ijhydene.2019.06.162

[90] Sazali N, Salleh WNW, Ismail AF. Carbon tubular membranes from nanocrystalline cellulose blended with P84 co-polyimide for H_2 and He separation. Int J Hydrogen Energy 2017;42(15):9952–7.
[91] Richter H, et al. High-flux carbon molecular sieve membranes for gas separation. Angew Chem Int Ed 2017;56(27):7760–3.
[92] Tseng H-H, Shiu P-T, Lin Y-S. Effect of mesoporous silica modification on the structure of hybrid carbon membrane for hydrogen separation. Int J Hydrogen Energy 2011;36(23):15352–63.
[93] Teixeira M, et al. Boehmite-phenolic resin carbon molecular sieve membranes—permeation and adsorption studies. Chem Eng Res Des 2014;92(11):2668–80.
[94] Yoda S, et al. Preparation of a platinum and palladium/polyimide nanocomposite film as a precursor of metal-doped carbon molecular sieve membrane via supercritical impregnation. Chem Mater 2004;16(12):2363–8.
[95] Kumakiri I, et al. Influence of iron additive on the hydrogen separation properties of carbon molecular sieve membranes. Ind Eng Chem Res 2018;57(15):5370–7.
[96] Wang C, et al. An improvement of the hydrogen permeability of C/Al2O3 membranes by palladium deposition into the pores. Int J Hydrogen Energy 2013;38(25):10819–25.
[97] Wey M-Y, Tseng H-H, Chiang C-k. Effect of MFI zeolite intermediate layers on gas separation performance of carbon molecular sieve (CMS) membranes. J Membr Sci 2013;446:220–9.
[98] Tseng H-H, et al. Enhanced H_2/CH_4 and H_2/CO_2 separation by carbon molecular sieve membrane coated on titania modified alumina support: effects of TiO2 intermediate layer preparation variables on interfacial adhesion. J Membr Sci 2016;510:391–404.
[99] Tseng H-H, Itta AK. Modification of carbon molecular sieve membrane structure by self-assisted deposition carbon segment for gas separation. J Membr Sci 2012;389:223–33.
[100] Dai Z, et al. Combination of ionic liquids with membrane technology: a new approach for CO_2 separation. J Membr Sci 2016;497:1–20.
[101] Bernhardsen IM, Knuutila HK. A review of potential amine solvents for CO_2 absorption process: absorption capacity, cyclic capacity and pKa. Int J Greenhouse Gas Contr 2017;61:27–48.
[102] Gouedard C, et al. Amine degradation in CO_2 capture. I. A review. Int J Greenhouse Gas Contr 2012;10:244–70.
[103] Bakonyi P, Nemestóthy N, Bélafi-Bakó K. Biohydrogen purification by membranes: an overview on the operational conditions affecting the performance of non-porous, polymeric and ionic liquid based gas separation membranes. Int J Hydrogen Energy 2013;38(23):9673–87.
[104] Tome LC, Marrucho IM. Ionic liquid-based materials: a platform to design engineered CO_2 separation membranes. Chem Soc Rev 2016;45(10):2785–824.
[105] Sasikumar B, Arthanareeswaran G, Ismail AF. Recent progress in ionic liquid membranes for gas separation. J Mol Liq 2018;266:330–41.
[106] Wang J, et al. Recent development of ionic liquid membranes. Green Energy Environ 2016;1(1):43–61.
[107] Sadeghpour M, Yusoff R, Aroua MK. Polymeric ionic liquids (PILs) for CO_2 capture. Rev Chem Eng 2017;33(2):183–200.
[108] Yan X, et al. Ionic liquids combined with membrane separation processes: a review. Separ Purif Technol 2019;222:230–53.
[109] Rynkowska E, Fatyeyeva K, Kujawski W. Application of polymer-based membranes containing ionic liquids in membrane separation processes: a critical review. Rev Chem Eng 2018;34(3):341–63.
[110] Zulfiqar S, Sarwar MI, Mecerreyes D. Polymeric ionic liquids for CO_2 capture and separation: potential, progress and challenges. Polym Chem 2015;6(36):6435–51.
[111] Kárászová M, et al. Progress in separation of gases by permeation and liquids by pervaporation using ionic liquids: a review. Separ Purif Technol 2014;132:93–101.
[112] Aghaie M, Rezaei N, Zendehboudi S. A systematic review on CO_2 capture with ionic liquids: current status and future prospects. Renew Sustain Energy Rev 2018;96:502–25.
[113] Hayes R, Warr GG, Atkin R. Structure and nanostructure in ionic liquids. Chem Rev 2015;115(13):6357–426.
[114] Finotello A, et al. Room-temperature ionic Liquids: temperature dependence of gas solubility selectivity. Ind Eng Chem Res 2008;47(10):3453–9.
[115] Zhao W, et al. Membrane liquid loss mechanism of supported ionic liquid membrane for gas separation. J Membr Sci 2012;411–412:73–80.
[116] Lodge TP. A unique platform for materials design. Science 2008;321(5885):50–1.
[117] Mulder M. Chapter V - transport in membranes. In: Basic principles of membrane technology. Springer; 1996.
[118] Hanioka S, et al. CO_2 separation facilitated by task-specific ionic liquids using a supported liquid membrane. J Membr Sci 2008;314(1):1–4.
[119] Lee JH, et al. Facilitated CO_2 transport membranes utilizing positively polarized copper nanoparticles. Chem Commun 2012;48(43):5298–300.
[120] Valencia-Marquez D, Flores-Tlacuahuac A, Ricardez-Sandoval L. Technoeconomic and dynamical analysis of a CO_2 capture pilot-scale plant using ionic liquids. Ind Eng Chem Res 2015;54(45):11360–70.
[121] Myers C, et al. High temperature separation of carbon dioxide/hydrogen mixtures using facilitated supported ionic liquid membranes. J Membr Sci 2008;322(1):28–31.
[122] Karousos DS, et al. Effect of a cyclic heating process on the CO_2/N_2 separation performance and structure of a ceramic nanoporous membrane supporting the ionic liquid 1-methyl-3-octylimidazolium tricyanomethanide. Separ Purif Technol 2018;200:11–22.
[123] Liang L, Gan Q, Nancarrow P. Composite ionic liquid and polymer membranes for gas separation at elevated temperatures. J Membr Sci 2014;450:407–17.
[124] Neves LA, et al. Separation of biohydrogen by supported ionic liquid membranes. Desalination 2009;240(1):311–5.
[125] Cserjési P, Nemestóthy N, Bélafi-Bakó K. Gas separation properties of supported liquid membranes prepared with unconventional ionic liquids. J Membr Sci 2010;349(1):6–11.
[126] Liu Z, et al. CO_2 separation by supported ionic liquid membranes and prediction of separation performance. Int J Greenhouse Gas Contr 2016;53:79–84.
[127] Neves LA, Crespo JG, Coelhoso IM. Gas permeation studies in supported ionic liquid membranes. J Membr Sci 2010;357(1):160–70.
[128] Wickramanayake S, et al. Mechanically robust hollow fiber supported ionic liquid membranes for CO_2 separation applications. J Membr Sci 2014;470:52–9.
[129] Chen HZ, Li P, Chung T-S. PVDF/ionic liquid polymer blends with superior separation performance for removing CO_2 from hydrogen and flue gas. Int J Hydrogen Energy 2012;37(16):11796–804.
[130] Bernardo P, et al. Gas transport properties of Pebax®/room temperature ionic liquid gel membranes. Separ Purif Technol 2012;97:73–82.
[131] Kanehashi S, et al. CO_2 separation properties of a glassy aromatic polyimide composite membranes containing high-content 1-butyl-3-methylimidazolium bis(trifluoromethylsulfonyl)imide ionic liquid. J Membr Sci 2013;430:211–22.

Please cite this article as: Bernardo G et al., Recent advances in membrane technologies for hydrogen purification, International Journal of Hydrogen Energy, https://doi.org/10.1016/j.ijhydene.2019.06.162

[132] Rabiee H, Ghadimi A, Mohammadi T. Gas transport properties of reverse-selective poly(ether-b-amide6)/[Emim][BF4] gel membranes for CO_2/light gases separation. J Membr Sci 2015;476:286–302.
[133] Jansen JC, et al. High ionic liquid content polymeric gel membranes: preparation and performance. Macromolecules 2011;44(1):39–45.
[134] Friess K, et al. High ionic liquid content polymeric gel membranes: correlation of membrane structure with gas and vapour transport properties. J Membr Sci 2012;415–416:801–9.
[135] Jansen JC, et al. Gas transport properties and pervaporation performance of fluoropolymer gel membranes based on pure and mixed ionic liquids. Separ Purif Technol 2013;109:87–97.
[136] Couto RM, et al. Development of ion-jelly® membranes. Separ Purif Technol 2013;106:22–31.
[137] Bara JE, et al. Synthesis and performance of polymerizable room-temperature ionic liquids as gas separation membranes. Ind Eng Chem Res 2007;46(16):5397–404.
[138] Wiesenauer EF, et al. Imidazolium-containing, hydrophobic–ionic–hydrophilic ABC triblock copolymers: synthesis, ordered phase-separation, and supported membrane fabrication. Soft Matter 2013;9(33):7923–7.
[139] Zarca G, et al. Synthesis and gas separation properties of poly(ionic liquid)-ionic liquid composite membranes containing a copper salt. J Membr Sci 2016;515:109–14.
[140] Cowan MG, et al. Phosphonium-based poly(Ionic liquid) membranes: the effect of cation alkyl chain length on light gas separation properties and Ionic conductivity. J Membr Sci 2016;498:408–13.
[141] Mittenthal MS, et al. Ionic polyimides: hybrid polymer architectures and composites with ionic liquids for advanced gas separation membranes. Ind Eng Chem Res 2017;56(17):5055–69.
[142] Deville HSC, Troost L. Sur la Perméabilité du Fer à Haute Température. Compt Rendus 1863:965–7.
[143] Graham T. On the absorption and dialytic separation of gases by colloid septa. Phil R Soc Lond 1866;156:399–439.
[144] Juenker DW, Swaay MV, Birchenall CE. On the use of palladium diffusion membranes for the purification of hydrogen. Rev Sci Instrum 1955;26(9). 888-888.
[145] Doukelis A, et al., editors. Palladium membrane technology for hydrogen production, carbon capture and other applications: principles, energy production and other applications. Woodhead publishing series in energy. Woodhead Publishing; 2014.
[146] Timofeev NI, Berseneva FN, Makarov VM. New palladium-based membrane alloys for separation of gas mixtures to generate ultrapure hydrogen. Int J Hydrogen Energy 1994;19(11):895–8.
[147] Nakatsuji H, Hada M. Interaction of a hydrogen molecule with palladium. J Am Chem Soc 1985;107(26):8264–6.
[148] Huang Y, et al. Characterization of the adhesion of thin palladium membranes supported on tubular porous ceramics. Thin Solid Films 2007;515(13):5233–40.
[149] Okazaki J, et al. Importance of the support material in thin palladium composite membranes for steady hydrogen permeation at elevated temperatures. Phys Chem Chem Phys 2009;11(38):8632–8.
[150] Mardilovich IP, Engwall E, Ma YH. Dependence of hydrogen flux on the pore size and plating surface topology of asymmetric Pd-porous stainless steel membranes. Desalination 2002;144(1):85–9.
[151] Gao H, et al. Chemical stability and its improvement of palladium-based metallic membranes. Ind Eng Chem Res 2004;43(22):6920–30.
[152] Li A, Liang W, Hughes R. The effect of carbon monoxide and steam on the hydrogen permeability of a Pd/stainless steel membrane. J Membr Sci 2000;165(1):135–41.
[153] Hou K, Hughes R. The effect of external mass transfer, competitive adsorption and coking on hydrogen permeation through thin Pd/Ag membranes. J Membr Sci 2002;206(1):119–30.
[154] Li H, et al. PdC formation in ultra-thin Pd membranes during separation of H2/CO mixtures. J Membr Sci 2007;299(1):130–7.
[155] Murmura MA, Sheintuch M. Permeance inhibition of Pd-based membranes by competitive adsorption of CO: membrane size effects and first principles predictions. Chem Eng J 2018;347:301–12.
[156] O'Brien CP, Lee IC. The interaction of CO with PdCu hydrogen separation membranes: an operando infrared spectroscopy study. Cataly Today 2017. https://doi.org/10.1016/j.cattod.2017.09.039 (in press).
[157] Burke ML, Madix RJ. Hydrogen on Pd(100)-S: the effect of sulfur on precursor mediated adsorption and desorption. Surf Sci 1990;237(1):1–19.
[158] Castro FJ, Meyer G, Zampieri G. Effects of sulfur poisoning on hydrogen desorption from palladium. J Alloy Comp 2002;330–332:612–6.
[159] O'Brien CP, et al. Inhibition of hydrogen transport through Pd and $Pd_{47}Cu_{53}$ membranes by H_2S at 350°C. J Membr Sci 2010;349(1):380–4.
[160] Chen CH, Ma YH. The effect of H_2S on the performance of Pd and Pd/Au composite membrane. J Membr Sci 2010;362(1–2):535–44.
[161] Feng W, et al. Influence of hydrogen sulfide and redox reactions on the surface properties and hydrogen permeability of Pd membranes. Energies 2018;11(5):1127.
[162] Spallina V, et al. Techno-economic assessment of membrane assisted fluidized bed reactors for pure H_2 production with CO_2 capture. Energy Convers Manag 2016;120:257–73.
[163] Roses L, et al. Techno-economic assessment of membrane reactor technologies for pure hydrogen production for fuel cell vehicle fleets. Energy Fuel 2013;27(8):4423–31.
[164] O'Donnell L, Maine E. Assessing development and commercialization priorities for a novel hydrogen production process through technical-economic cost modeling. Transl Mater Res 2015;2(1):016001.
[165] Alique D, et al. Review of supported Pd-based membranes preparation by electroless plating for ultra-pure hydrogen production. Membranes 2018;8(1):5.
[166] Conde JJ, Maroño M, Sánchez-Hervás JM. Pd-based membranes for hydrogen separation: review of alloying elements and their influence on membrane properties. Separ Purif Rev 2017;46(2):152–77.
[167] Rahimpour MR, et al. Palladium membranes applications in reaction systems for hydrogen separation and purification: a review. Chem Eng Proc Proc Intensificat 2017;121:24–49.
[168] Zhang K, Way JD. Palladium-copper membranes for hydrogen separation. Separ Purif Technol 2017;186:39–44.
[169] Li H, Caravella A, Xu HY. Recent progress in Pd-based composite membranes. J Mater Chem 2016;4(37):14069–94.
[170] Al-Mufachi NA, Rees NV, Steinberger-Wilkens R. Hydrogen selective membranes: a review of palladium-based dense metal membranes. Renew Sustain Energy Rev 2015;47:540–51.
[171] Hatlevik Ø, et al. Palladium and palladium alloy membranes for hydrogen separation and production: history, fabrication strategies, and current performance. Separ Purif Technol 2010;73(1):59–64.
[172] Adams BD, Chen A. The role of palladium in a hydrogen economy. Mater Today 2011;14(6):282–9.

Please cite this article as: Bernardo G et al., Recent advances in membrane technologies for hydrogen purification, International Journal of Hydrogen Energy, https://doi.org/10.1016/j.ijhydene.2019.06.162

[173] Roa F, et al. Palladium-copper and palladium-gold alloy composite membranes for hydrogen separations. In: Bose AC, editor. Inorganic membranes for energy and environmental applications. New York, NY: Springer New York; 2009. p. 221–39.
[174] Lee SM, et al. Palladium/ruthenium composite membrane for hydrogen separation from the off-gas of solar cell production via chemical vapor deposition. J Membr Sci 2017;541:1–8.
[175] Melendez J, et al. Effect of Au addition on hydrogen permeation and the resistance to H_2S on Pd-Ag alloy membranes. J Membr Sci 2017;542:329–41.
[176] Jia H, et al. High-temperature stability of Pd alloy membranes containing Cu and Au. J Membr Sci 2017;544:151–60.
[177] Fontana AD, et al. Hydrogen permeation and surface properties of PdAu and PdAgAu membranes in the presence of CO, CO_2 and H_2S. J Membr Sci 2018;563:351–9.
[178] Sanz R, et al. Hydrogen production in a Pore-Plated Pd-membrane reactor: experimental analysis and model validation for the Water Gas Shift reaction. Int J Hydrogen Energy 2015;40(8):3472–84.
[179] Martinez-Diaz D, et al. H_2 permeation increase of electroless pore-plated Pd/PSS membranes with CeO_2 intermediate barriers. Separ Purif Technol 2019;216:16–24.
[180] Zhao C, Xu H, Goldbach A. Duplex Pd/ceramic/Pd composite membrane for sweep gas-enhanced CO_2 capture. J Membr Sci 2018;563:388–97.
[181] Yu J, et al. Synthesis of a zeolite membrane as a protective layer on a metallic Pd composite membrane for hydrogen purification. J Mater Chem 2015;3(9):5000–6.
[182] Abate S, et al. Influence of zeolite protective overlayer on the performances of Pd thin film membrane on tubular asymmetric alumina supports. Ind Eng Chem Res 2016;55(17):4948–59.
[183] Guo Y, et al. Deposition of TS-1 zeolite film on palladium membrane for enhancement of membrane stability. Int J Hydrogen Energy 2017;42(44):27111–21.
[184] Yu J, et al. Controllable growth of defect-free zeolite protective layer on the surface of Pd membrane for chemical stability enhancement. Microporous Mesoporous Mater 2017;244:119–26.
[185] Yu J, et al. Confined and in-situ zeolite synthesis: a novel strategy for defect reparation over dense Pd membranes for hydrogen separation. Separ Purif Technol 2017;184:43–53.
[186] Arratibel A, et al. Development of Pd-based double-skinned membranes for hydrogen production in fluidized bed membrane reactors. J Membr Sci 2018;550:536–44.
[187] Arratibel A, et al. Attrition-resistant membranes for fluidized-bed membrane reactors: double-skin membranes. J Membr Sci 2018;563:419–26.
[188] Helmi A, Gallucci F, van Sint Annaland M. Resource scarcity in palladium membrane applications for carbon capture in integrated gasification combined cycle units. Int J Hydrogen Energy 2014;39(20):10498–506.
[189] Fernandez E, et al. Development of highly permeable ultra-thin Pd-based supported membranes. Chem Eng J 2016;305:149–55.
[190] Fernandez E, et al. Preparation and characterization of metallic supported thin Pd–Ag membranes for hydrogen separation. Chem Eng J 2016;305:182–90.
[191] Melendez J, et al. Preparation and characterization of ceramic supported ultra-thin (~1μm) Pd-Ag membranes. J Membr Sci 2017;528:12–23.
[192] Kim DH, et al. Effect of PBI-HFA surface treatments on Pd/PBI-HFA composite gas separation membranes. Int J Hydrogen Energy 2017;42(36):22915–24.
[193] Kong SY, et al. Ultrathin layered Pd/PBI–HFA composite membranes for hydrogen separation. Separ Purif Technol 2017;179:486–93.
[194] Dunbar ZW, Lee IC. Effects of elevated temperatures and contaminated hydrogen gas mixtures on novel ultrathin palladium composite membranes. Int J Hydrogen Energy 2017;42(49):29310–9.
[195] Liu LC, et al. Solubility, diffusivity, and permeability of hydrogen at PdCu phases. J Membr Sci 2017;542:24–30.
[196] Liu LC, et al. Fundamental effects of Ag alloying on hydrogen behaviors in PdCu. J Membr Sci 2018;550:230–7.
[197] Kumar N, et al. Microscopic insights into hydrogen permeation through a model PdCu membrane from first-principles investigations. J Phys Chem C 2018;122(24):12920–33.
[198] Zhao M, Sloof WG, Böttger AJ. Modelling of surface segregation for palladium alloys in vacuum and gas environments. Int J Hydrogen Energy 2018;43(4):2212–23.
[199] Maget HJR. In: Process for gas purification, U.S.P. Office; 1970. USA.
[200] McEvoy JE, et al. Hydrogen purification using modified fuel cell process. Ind Eng Chem Process Des Dev 1965;4(1):1–3.
[201] Rosli RE, et al. A review of high-temperature proton exchange membrane fuel cell (HT-PEMFC) system. Int J Hydrogen Energy 2017;42(14):9293–314.
[202] Wong CY, et al. Additives in proton exchange membranes for low- and high-temperature fuel cell applications: a review. Int J Hydrogen Energy 2019;44(12):6116–35.
[203] Omrani R, Shabani B. Review of gas diffusion layer for proton exchange membrane-based technologies with a focus on unitised regenerative fuel cells. Int J Hydrogen Energy 2019;44(7):3834–60.
[204] Dafalla AM, Jiang F. Stresses and their impacts on proton exchange membrane fuel cells: a review. Int J Hydrogen Energy 2018;43(4):2327–48.
[205] Haque MA, et al. Acid doped polybenzimidazoles based membrane electrode assembly for high temperature proton exchange membrane fuel cell: a review. Int J Hydrogen Energy 2017;42(14):9156–79.
[206] Fishel K, et al. Electrochemical hydrogen pumping. In: Li Qingfeng, et al., editors. High temperature polymer electrolyte membrane fuel cells. Switzerland: Springer; 2016. p. 527–40.
[207] Pasierb P, Rekas M. High-temperature electrochemical hydrogen pumps and separators. Int J Electrochem 2011;2011:10.
[208] Onda K, et al. Separation and compression characteristics of hydrogen by use of proton exchange membrane. J Power Sources 2007;164(1):1–8.
[209] Dupuis A-C. Proton exchange membranes for fuel cells operated at medium temperatures: materials and experimental techniques. Prog Mater Sci 2011;56(3):289–327.
[210] Alberti G, et al. Polymeric proton conducting membranes for medium temperature fuel cells (110–160°C). J Membr Sci 2001;185(1):73–81.
[211] Phair JW, Badwal SPS. Review of proton conductors for hydrogen separation. Ionics 2006;12(2):103–15.
[212] Lee HK, et al. Hydrogen separation using electrochemical method. J Power Sources 2004;132(1):92–8.
[213] Gardner CL, Ternan M. Electrochemical separation of hydrogen from reformate using PEM fuel cell technology. J Power Sources 2007;171(2):835–41.
[214] Abdulla A, et al. Efficiency of hydrogen recovery from reformate with a polymer electrolyte hydrogen pump. AIChE J 2011;57(7):1767–79.

Please cite this article as: Bernardo G et al., Recent advances in membrane technologies for hydrogen purification, International Journal of Hydrogen Energy, https://doi.org/10.1016/j.ijhydene.2019.06.162

[215] Hao Y, et al. Characterization of an electrochemical hydrogen pump with internal humidifier and dead-end anode channel. Int J Hydrogen Energy 2016;41(32):13879–87.
[216] Sedlak JM, Austin JF, LaConti AB. Hydrogen recovery and purification using the solid polymer electrolyte electrolysis cell. Int J Hydrogen Energy 1981;6(1):45–51.
[217] Barbir F, Görgün H. Electrochemical hydrogen pump for recirculation of hydrogen in a fuel cell stack. J Appl Electrochem 2007;37(3):359–65.
[218] Grigoriev SA, et al. Description and characterization of an electrochemical hydrogen compressor/concentrator based on solid polymer electrolyte technology. Int J Hydrogen Energy 2011;36(6):4148–55.
[219] Casati C, et al. Some fundamental aspects in electrochemical hydrogen purification/compression. J Power Sources 2008;180(1):103–13.
[220] Kusoglu A, Weber AZ. New insights into perfluorinated sulfonic-acid ionomers. Chem Rev 2017;117(3):987–1104.
[221] Araya SS, et al. A comprehensive review of PBI-based high temperature PEM fuel cells. Int J Hydrogen Energy 2016;41(46):21310–44.
[222] Li Q, et al. High temperature proton exchange membranes based on polybenzimidazoles for fuel cells. Prog Polym Sci 2009;34(5):449–77.
[223] Subianto S. Recent advances in polybenzimidazole/phosphoric acid membranes for high-temperature fuel cells. Polym Int 2014;63(7):1134–44.
[224] Perry KA, Eisman GA, Benicewicz BC. Electrochemical hydrogen pumping using a high-temperature polybenzimidazole (PBI) membrane. J Power Sources 2008;177(2):478–84.
[225] Thomassen M, Sheridan E, Kvello J. Electrochemical hydrogen separation and compression using polybenzimidazole (PBI) fuel cell technology. J Nat Gas Sci Eng 2010;2(5):229–34.
[226] Kim SJ, et al. Characterizations of polybenzimidazole based electrochemical hydrogen pumps with various Pt loadings for H2/CO2 gas separation. Int J Hydrogen Energy 2013;38(34):14816–23.
[227] Polybenzimidazole (PBI) - polymer properties database [cited 2019 12th June]; Available from: https://polymerdatabase.com.
[228] Gebel G. Structure of membranes for fuel cells: SANS and SAXS analyses of sulfonated PEEK membranes and solutions. Macromolecules 2013;46(15):6057–66.
[229] Kreuer KD. On the development of proton conducting polymer membranes for hydrogen and methanol fuel cells. J Membr Sci 2001;185(1):29–39.
[230] Wu X, et al. Electrochemical hydrogen pump with SPEEK/CrPSSA semi-interpenetrating polymer network proton exchange membrane for H_2/CO_2 separation. ACS Sustain Chem Eng 2014;2(1):75–9.
[231] Huang S, et al. Coupling hydrogen separation with butanone hydrogenation in an electrochemical hydrogen pump with sulfonated poly (phthalazinone ether sulfone ketone) membrane. J Power Sources 2016;327:178–86.
[232] Rico-Zavala A, et al. Synthesis and characterization of composite membranes modified with Halloysite nanotubes and phosphotungstic acid for electrochemical hydrogen pumps. Renew Energy 2018;122:163–72.
[233] Kim G, et al. Understanding the conduction mechanism of the protonic conductor CsH_2PO_4 by solid-state NMR spectroscopy. J Phys Chem C 2013;117(13):6504–15.
[234] Botez CE, et al. High pressure synchrotron x-ray diffraction studies of superprotonic transitions in phosphate solid acids. Solid State Ionics 2012;213:58–62.
[235] Botez CE, et al. High-temperature phase transitions in CsH2PO4 under ambient and high-pressure conditions: a synchrotron x-ray diffraction study. J Chem Phys 2007;127(19):194701.
[236] Haile SM, et al. Solid acid proton conductors: from laboratory curiosities to fuel cell electrolytes. Faraday Discuss 2007;134:17–39.
[237] Papandrew AB, et al. Electrochemical hydrogen separation via solid acid membranes. In: Zhou XD, et al., editors. Electrochemical synthesis of fuels 2; 2013. p. 33–8.
[238] Papandrew AB, Zawodzinski TA. Nickel catalysts for hydrogen evolution from CsH_2PO_4. J Power Sources 2014;245:171–4.
[239] Kreuer KD. Proton-conducting oxides. Annu Rev Mater Res 2003;33(1):333–59.
[240] Iwahara H, et al. High temperature type protonic conductor based on $SrCeO_3$ and its application to the extraction of hydrogen gas. Solid State Ionics 1986;18–19:1003–7.
[241] Iwahara H. Hydrogen pumps using proton-conducting ceramics and their applications. Solid State Ionics 1999;125(1):271–8.
[242] Matsumoto H, Iida Y, Iwahara H. Current efficiency of electrochemical hydrogen pumping using a high-temperature proton conductor SrCe0.95Yb0.05O3–α. Solid State Ionics 2000;127(3):345–9.
[243] Sakai T, et al. High performance of electroless-plated platinum electrode for electrochemical hydrogen pumps using strontium-zirconate-based proton conductors. Electrochim Acta 2008;53(28):8172–7.
[244] Sakai T, et al. Performance of palladium electrode for electrochemical hydrogen pump using strontium-zirconate-based proton conductors. Ionics 2009;15(6):665.
[245] Sakai T, et al. Electrochemical hydrogen pumps using Ba doped $LaYbO_3$ type proton conducting electrolyte. Int J Hydrogen Energy 2013;38(16):6842–7.
[246] Choi J, et al. High-performance ceramic composite electrodes for electrochemical hydrogen pump using protonic ceramics. Int J Hydrogen Energy 2017;42(18):13092–8.
[247] Messaoudani Zl, et al. Hazards, safety and knowledge gaps on hydrogen transmission via natural gas grid: a critical review. Int J Hydrogen Energy 2016;41(39):17511–25.
[248] Melaina MW, Antonia O, Penev M. Blending hydrogen into natural gas pipeline networks: a review of key issues. NREL - National Renewable Energy Laboratory; 2013.
[249] Demir ME, Dincer I. Cost assessment and evaluation of various hydrogen delivery scenarios. Int J Hydrogen Energy 2018;43(22):10420–30.
[250] Gondal IA. Hydrogen integration in power-to-gas networks. Int J Hydrogen Energy 2019;44(3):1803–15.
[251] Wang B, et al. An MILP model for the reformation of natural gas pipeline networks with hydrogen injection. Int J Hydrogen Energy 2018;43(33):16141–53.

Please cite this article as: Bernardo G et al., Recent advances in membrane technologies for hydrogen purification, International Journal of Hydrogen Energy, https://doi.org/10.1016/j.ijhydene.2019.06.162